A STUDY OF SEMI-LAGRANGIAN ADVECTION SCHEMES USING LEAST SQUARES INTERPOLATION

a dissertation
submitted to the department of geophysics
niels bohr institute for astronomy, physics and geophysics
University of Copenhagen
in partial fulfillment of the requirements
for the degree of
Master of Science

Peter Hjort Lauritzen
January 2002

Preface

The group of scientists assembled at the WCRP symposium on global transport models held in Bermuda in December 1990 [WCRP, 1990] recognized that the use of the semi-Lagrangian technique is desirable. Judging from the continuous stream of articles published each year on the topic, one may safely conclude that the desirability of the semi-Lagrangian approach has *not* lost its glance during the last decade. Despite the huge amount of work in the field, replacing conventional Lagrange interpolation with a least squares polynomial fit seems unexplored. Therefore my supervisor, professor J. R. Bates, suggested an investigation of the numerical consequences of employing least squares interpolation. After the preliminary analysis I independently constructed a more general semi-Lagrangian scheme based on Taylor series expansions. Accuracy requirements were chosen to leave one degree of freedom which may be exploited to improve desirable properties. The conventional Lagrange interpolator, as well as the least squares one, are special cases of this more general scheme. The investigation of the least squares approach and the extension to a more general scheme is the subject of this study. The analysis is directed towards applications in atmospheric transport problems.

Acknowledgments

First of all I would like to thank my supervisor, Professor J. R. Bates, for providing unique supervision as well as encouraging me to participate in inspiring summer schools. Furthermore, I thank him for awakening my interest in numerical fluid dynamics during one of his courses. I would also like to thank the Department of Geophysics of the University of Bergen, especially Professor S. Grønås, for support during the final phase of this study.

Peter Hjort Lauritzen, January 2002
University of Copenhagen
Niels Bohr Institute of Astronomy, Physics and Geophysics
Department of Geophysics

Abstract

The choice of interpolation method in a semi-Lagrangian scheme is crucial to its performance. Given the number of grid points one is considering to use for the interpolation, it does not necessarily follow that maximum formal accuracy should give the best results. Relaxing one order of accuracy creates one degree of freedom. Varying this free parameter generates a family of stable integration schemes of which conventional semi-Lagrangian schemes and schemes using least squares interpolation are special cases. This permits a simultaneous analysis of the properties of the least squares approach and other schemes of the same order of accuracy. The analysis is restricted to the one-dimensional case.

"To those who do not know mathematics it is difficult to get across a real feeling as to the beauty, the deepest beauty, of nature. ... If you want to learn about nature, to appreciate nature, it is necessary to understand the language that she speaks in."

Richard P. Feynman
The Character of Physical Law

Contents

Chapter 1

Introduction

It seems reasonable to start off by requiring that any numerical algorithm designed for solving geophysical flow problems should, before anything else, get advection right. Hence, investigating an unexplored numerical algorithm evidently restricts the preliminary analysis to the unforced transport equation

$$\frac{D\psi}{Dt} = \frac{\partial \psi}{\partial t} + \mathbf{v} \cdot \nabla \psi = 0\,, \tag{1.1}$$

defined on a domain $\mathcal{D} \subseteq \mathbb{R}^m$, where $\psi(\mathbf{x}, t)$ is a fluid variable. The variables $\mathbf{x} \in \mathbb{R}^m$ and $t \in \mathbb{R}$ have their usual meaning of spatial and temporal coordinates. The predetermined velocity of the fluid is denoted $\mathbf{v} \in \mathbb{R}^m$. Since $\frac{D\psi}{Dt} = 0$, ψ is constant along the trajectories of the flow. Despite the simple analytical solution, it has proven to be a highly challenging task to design satisfactory transport schemes for general applications (see for example [Rood, 1987] for a review of many numerical approaches[1]). It is safe to conclude that there exist no universal best choice. Since the seminal work of Robert [Robert, 1981], the semi-Lagrangian methods have attracted increasing attention, leading to substantial literature over the past decades. Since the extensive review of [Staniforth and Côté, 1991] many new and interesting semi-Lagrangian algorithms have been developed. It is not the purpose of this section to try to update the excellent work of Staniforth and Côté, but rather to provide a brief overview of

[1] note that real applications to atmospheric transport problems reveal that the conclusions of [Rood, 1987] were, at least naive, if not wrong [Lin and Rood, 1996]

some conventional and more recent semi-Lagrangian methods.

Traditionally semi-Lagrangian schemes were finite-difference schemes derived in a Lagrangian framework. That is no longer the case. For example, the term "semi-Lagrangian" has extended into the world of finite volume methods. Existing Eulerian finite volume methods have been extended to a formulation that can be stable under large Courant number. See for example the semi-Lagrangian extensions of the piecewise parabolic method (PPM) [Rancic, 1992], [Rancic, 1995] and the flux-form conservative semi-Lagrangian scheme in [Lin and Rood, 1996]. In the sense of meteorological terminology, these schemes are termed semi-Lagrangian, although they are quite different from the traditional semi-Lagrangian approach. Also the CIP-method (cubic interpolated propagation) has recently been developed into a semi-Lagrangian and conservative form [Yabe et al., 2001]. These are just a few examples of a longer list of semi-Lagrangian extensions.

It is beyond the scope of this introduction to discuss these newer developments which extend the traditional conception of semi-Lagrangian schemes. Hence, we will formally exclude finite volume methods and other non-finite-difference approaches. However, one should be aware of alternative semi-Lagrangian methods, since they intrinsically offer a combination of properties which are not *a priori* in the traditional semi-Lagrangian framework.

1.1 Finite difference schemes

Assume that the domain $\mathcal{D}$ is discretized into some kind of computational grid. [Smolarkiewicz and Pudykiewicz, 1992] present a very elegant and unifying way of interpreting finite difference approaches for solving the advection equation:

From Stokes' theorem and (1.1), the fluid variable ψ satisfies

$$\psi(\mathbf{x}_1, t_1) = \psi(\mathbf{x}_0, t_0) + \int_{\mathcal{C}} (d\mathbf{x} - \mathbf{v}\, dt) \cdot \nabla\psi\,, \tag{1.2}$$

where $\mathcal{C}$ denotes an arbitrary contour connecting the two points $(\mathbf{x}_0, t_0)$ and $(\mathbf{x}_1, t_1)$ of a space-time continuum $\mathcal{D} \times \mathbb{R}$. For computational reasons, it is convenient to let

$\mathbf{x}_1$ be a grid point on the computational mesh but it is of course not a requirement. Similarly, $\mathbf{x}_0$ may be any point in the time-plane $t = t_0$. The formal solution of (1.2) unifies the conventional Eulerian and Lagrangian approaches: Selecting $\mathbf{x}_0 = \mathbf{x}_1$ results in the purely Eulerian integral of (1.1), whereas selecting $\mathbf{x}_0 = \mathbf{x}_*$, where $(\mathbf{x}_*, t_0)$ is the departure point of the trajectory arriving at $(\mathbf{x}_1, t_1)$, more precisely

$$\mathbf{x}_* = \mathbf{x}_1 + \int_{t_1}^{t_0} \mathbf{v}(\mathbf{x}, t)\, dt\,, \tag{1.3}$$

leads to a purely Lagrangian integral. In essence, the Lagrangian method depends on accurate integration of (1.3) to obtain the previous position of the particle. Trajectory integration is discussed in [Smolarkiewicz and Pudykiewicz, 1992].

1.1.1 Conventional semi-Lagrangian schemes

The latter contour selection leads to the conventional semi-Lagrangian formulation when $\mathbf{x}_1$ is chosen to coincide with a grid point. Since the particle path is followed, the formal integral in (1.2) vanishes and the numerical problem is reduced to the approximation of $\psi(\mathbf{x}_*, t_0)$. Since the departure point $(\mathbf{x}_*, t_0)$ does not necessarily coincide with a point on the mesh, one has to invoke some kind of interpolation procedure in order to determine the value of $\psi(\mathbf{x}_*, t_0)$. Any consistent interpolation method known to the author provides a scheme which circumvents the Courant-Friedrichs-Lewy (CFL) stability condition typically required in Eulerian methods. Therefore the time step may be chosen based on accuracy considerations rather than stability[2]. Simultaneously we have the convenience of a regular mesh discretization in contrast to purely Lagrangian methods.

In the meteorological community the most widespread interpolation methods are cubic Lagrange interpolation (e.g.,[Bates and McDonald, 1982]) and cubic splines (e.g. [Purnell, 1976]; [Riishjgaard et al., 1998]). A remarkable fact about cubic splines is that they conserve mass exactly[3] for non-divergent flow fields [Bermejo, 1990]. This is normally not the case in conventional semi-Lagrangian schemes and the lack of it

[2] if the velocity field does vary rapidly instability may occur

[3] we assume that ψ is some mass specific quantity

is a matter of some concern. Since conventional semi-Lagrangian schemes are always cast in non-conservative form, it is very difficult to construct finite difference schemes which conserve mass without using post adjustment algorithms. Nevertheless, one should be aware of the fact that many so-called conservative schemes, derived in an Eulerian framework[4], are strictly conservative only if time is kept continuous. Therefore conservation is only accomplished with accuracy to the truncation error of the time differencing. However, for some applications (for example long term climate studies) mass conservation is often regarded as indispensable and hence inhibits many semi-Lagrangian schemes for direct use. Triggered by the intrinsic difficulties in deriving conservative formulations, *a posteriori* restoration methods have been developed. See for example the algorithm of [Priestly, 1993] which, by an iterative procedure, attempts to regain mass conservation.

An unfortunate property of conventional semi-Lagrangian schemes is that they tend to produce overshooting and undershooting in the interpolation of unsmooth regions. [Bermejo and Staniforth, 1992] suggested a simple and efficient algorithm which converts conventional semi-Lagrangian schemes to quasi-monotone ones. It does so by preventing the interpolation method in generating new extrema. Any *a posteriori* method may, however, interact undesirably with favorable properties of the scheme. A simple example is: Suppose cubic splines are used during the interpolation process. As mentioned before, cubic splines will provide a scheme which conserves mass. By implementing the quasi-conservative algorithm presented in [Bermejo and Staniforth, 1992], possible undershoots and overshoots will be clipped to prevent the generation of new extrema. As numerical values are altered, a possible consequence of employing the *a posteriori* method is that the conservation of mass is violated. Furthermore, clipping extrema in the data might produce results which resemble highly diffusive numerical schemes.

Alternatively, overshoots and undershoots can be eliminated by using shape-preserving interpolation. An example of an interpolation method which optionally is shape-preserving, is Hermite interpolation. Apart from interpolating the fluid variable (like any other interpolation method), the Hermite interpolator also interpolates

[4]flux form schemes

estimates of the derivatives of ψ at grid points. Appropriate constraints on the derivative estimate enforce monotonicity. See for example [Williamson and Rasch, 1989] and [Holnicki, 1995]. The results of the numerical tests using shape-preserving interpolators presented in the two articles just cited show slight mass increase or decrease when using the shape-preserving interpolator.

From the above discussion, one could naturally ask the question if it is possible to achieve monotonicity and mass conservation simultaneously without post adjustment. This seems very hard, if not impossible, within the conventional semi-Lagrangian framework. Using semi-Lagrangian finite volume schemes, however, one can achieve both conservation and monotonicity at the same time without *a posteriori* methods (see for example [Lin and Rood, 1996]).

Though the conventional semi-Lagrangian approach, in general, lacks intrinsic conservation and monotonicity properties, it has several virtues. Conventional semi-Lagrangian methods show very good phase speeds with little numerical dispersion. There is some damping due to interpolation, but it is fortunately very scale selective. Furthermore, conventional semi-Lagrangian schemes are associated with simplicity and relatively long time steps. Therefore they may be computationally more efficient than their Eulerian counterparts.

Apart from conventional semi-Lagrangian schemes and classical Eulerian methods, the freedom associated with the selection of $\mathbf{x}_0$ and $\mathcal{C}$ in (1.2) offers a variety of mixed Lagrangian-Eulerian formulations.

1.1.2 Mixed Lagrangian-Eulerian formulations

Over 15 years ago [Ritchie, 1986] formulated a *non-interpolating semi-Lagrangian scheme* by choosing an alternative trajectory in the space-time continuum. As in conventional semi-Lagrangian schemes, $\mathbf{x}_0$ was chosen as the departure point of the trajectory arriving at grid point $\mathbf{x}_1$. But instead of letting the contour $\mathcal{C}$ follow the Lagrangian particle trajectory, the contour was replaced by two vectors: One connecting the departure point and the nearest grid point in the $t = t_0$-plane, and the other is the residual. Integration of the first contour is exact, while the residual

is approximated by an Eulerian scheme. Hence non-interpolating. The scheme keeps the favorable property of a semi-Lagrangian scheme, circumvents the CFL limitations on the time step, and removes the computational damping inherent in conventional semi-Lagrangian schemes. It does, however, suffer problems if the velocity field varies too much ([Durran, 1998] p.327).

More recently [Smolarkiewicz and Pudykiewicz, 1992] presented a class of semi-Lagrangian schemes choosing another contour in the space-time continuum:

Let T denote the contour which is followed by the Lagrangian trajectory of a fluid parcel which arrives at grid point $(\mathbf{x}_1, t_1)$. Of course, integrating along this contour will result in a conventional semi-Lagrangian scheme. Let $\mathcal{C}'$ denote a trajectory in the t_0-plane connecting the departure point, $\mathbf{x}_*$, with the nearest grid point, $\mathbf{x}_0$. Choosing the union of these two trajectories, $T \cup \mathcal{C}'$, as the contour $\mathcal{C}$ in (1.2), it may be proved [Smolarkiewicz and Pudykiewicz, 1992] that the numerical solution can be represented by an advection equation, in which the local Courant number vector is replaced by a normalized displacement vector between $\mathbf{x}_0$ and $\mathbf{x}_*$. In principle, this transformed advection equation may be solved using any known algorithm. Since its "Courant" number is normalized, one may use algorithms whose time step is normally limited by the CFL stability criterion. In other words, we have a semi-Lagrangian scheme, in the sense that it supports long time steps, and the convenience of employing Eulerian schemes with favorable properties. For example, using a positive definite Eulerian scheme for solving the parametrized advection equation will result in a positive definite semi-Lagrangian algorithm.

It is quite clear that finite difference semi-Lagrangian schemes make up a broad spectrum of algorithms. Apparently, there are still an abundance of possibilities worthy of exploration providing a fertile breeding ground for this study. The work summarized in the thesis is entirely restricted to conventional semi-Lagrangian schemes. In the light of the current discussion, that means finite-difference schemes, where (1.2) is formally integrated along the contour T. At the root of the trajectory the value of the fluid variable is interpolated by using surrounding grid point values of ψ. As the use of a least squares polynomial fit for interpolation in a semi-Lagrangian

scheme seems unexplored in literature, the derivation of such schemes and their stability properties will be investigated first. An obvious further development within the least squares framework is to introduce weighting functions (weighted least squares), as it is often done when employing the least squares method in a statistical context. One may hope that proper choice of weighting functions enforces desired properties. These considerations are used as a motivator for the derivation of a more general semi-Lagrangian scheme which may be interpreted as an analysis of the possibilities in introducing weighted least squares. It is derived on the basis of accuracy considerations which are chosen to leave one free parameter[5]. This gives a lot of flexibility which may be taken to advantage in trying to formulate a scheme with improved overall properties. Furthermore, schemes using Lagrange interpolation and a least squares polynomial fit are special cases of the more general scheme. Therefore comparative analysis of the latter schemes is facilitated.

[5] the idea is certainly not new and has been explored in an Eulerian framework by [Takacs, 1985]

Chapter 2

Accuracy of Least Squares Schemes

When referring to *conventional* semi-Lagrangian schemes, we refer to semi-Lagrangian schemes using Lagrange interpolation to interpolate upstream points.

Consider the advection equation (1.1) in one dimension

$$\frac{\partial \psi}{\partial t} + U \cdot \frac{\partial \psi}{\partial x} = 0\,, \tag{2.1}$$

where the wind speed U is constant. Without loss of generality, we can assume $U > 0$. In order to formally define the approximation schemes, we assume equidistant spatial discretization with the step Δ; the time resolution step will be denoted Δt. Integrating over the trajectory of a particle, which arrives at grid point $I\Delta$ at time $(n+1)\Delta t$, equation (1.2) reduces to

$$\psi_I^{n+1} = \psi^n(x_*)\,,$$

where $\psi^n(x_*)$ is the value of ψ at the departure point, x_*, of the particle at time $n\Delta t$. Since U is constant, the departure point is simply

$$x_* = I\,\Delta - U\,\Delta t\,.$$

The value of $\psi^n(x_*)$ is obtained by performing a least squares polynomial fit using values of ψ at grid points nearest to x_*. We will refer to a linear fit when minimizing

the squared distance between a straight line and grid point values of ψ. For higher order fits the line is replaced by a parabola, third or fourth order polynomial. These are referred to as quadratic, cubic and quartic fits, respectively.

Notation In principle, this paragraph follows the one outlined in [McDonald, 1984]. Let N be the number of grid point values used by the interpolating polynomial. The non-negative integer p is chosen such that

$$\left(I - p - \tfrac{1}{2}\right) \cdot \Delta < x_* \leq \left(I - p + \tfrac{1}{2}\right) \cdot \Delta \,, \tag{2.2}$$

for schemes using an odd number of points (N odd). For schemes using an even number of grid point values for the interpolation (N even) choose p such that

$$(I - p - 1) \cdot \Delta < x_* \leq (I - p) \cdot \Delta \,. \tag{2.3}$$

If α and $\hat{\alpha}$ are defined as

$$\alpha \equiv U \frac{\Delta t}{\Delta} \,, \tag{2.4}$$

$$\hat{\alpha} \equiv \begin{cases} \alpha - p & N \text{ odd} \\ \alpha - p - \frac{1}{2} & N \text{ even,} \end{cases} \tag{2.5}$$

then p defined in equations (2.2) and (2.3) guarantee that

$$-\tfrac{1}{2} \leq \hat{\alpha} < \tfrac{1}{2} \,. \tag{2.6}$$

The relationship between the grid point axis and the value of $\hat{\alpha}$ for N odd is illustrated on the following diagram:

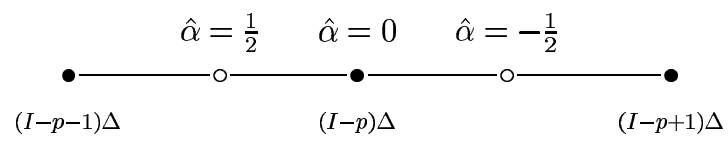

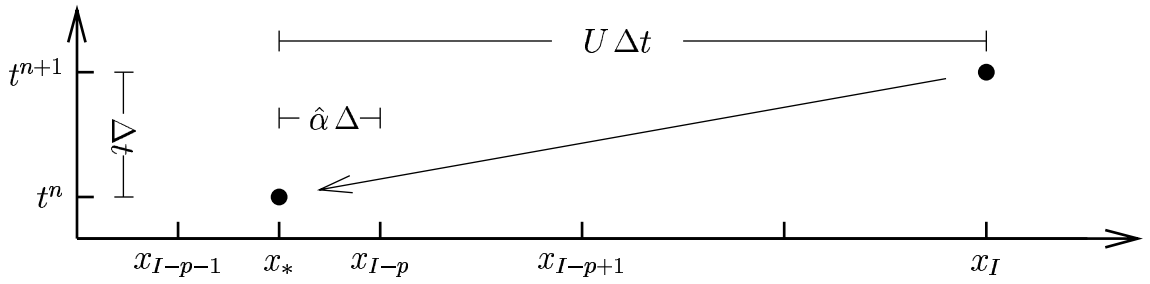

Figure 2.1: A space-time diagram illustrating the backward trajectory and the relevant notation for formulating the semi-Lagrangian solution in the case of N odd.

For N even we have

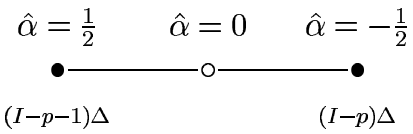

Having introduced appropriate notation figure 2.1 graphically illustrates the strategy behind the semi-Lagrangian approach using this notation.

2.1 Least squares schemes

The least squares method is explained in depth in appendix A.2. The basic idea is to find the polynomial which fits grid point values of ψ best in a least squares sense. That is to minimize the squared difference between grid point values of ψ and the fitting polynomial. Given the degree of the polynomial, we use a minimum number of points for the least squares approximation. That is, 3 points for a linear fit, 4 points for a quadratic fit, 5 points for a cubic fit and 6 points for a quartic fit[1]. Explicit formulas for the finite difference schemes, using first to fourth degree polynomial fits, are listed in table 2.1 (the formulas are derived in appendix A.2). By substituting

[1]note that if we use one point less in the fit we would perform a conventional Lagrange interpolation that fits grid point values exactly !

Taylor series expansions into the finite difference formulas, one may prove that the schemes are consistent and $(N-2)$th-order accurate[2].

2.2 Amplification factor

By performing a Von Neumann analysis we obtain the stability properties of the schemes. Assume a solution in the form

$$\phi_j^n = \Gamma^n \exp(i\, j\delta)\, \phi^0 ,$$

where $\delta \equiv k\Delta$ (k is the wave number), i is the imaginary unit and Γ is the amplification factor. By substituting the assumed solution into the finite difference formulas given in table 2.1 and defining $c \equiv 1 - \cos\delta$, the amplification factors can be written[3] as listed in table 2.2. The unconditional stability of the schemes can be proven by verifying that the expressions enclosed in the "curly" brackets, {}, in table 2.2 are non-negative for the range of values c and $\hat{\alpha}$ may take. Note that in the long wave limit, $\delta \to 0$, all amplification factors converge towards neutral amplification, $\|\Gamma\| \to 1$ (since $c \to 0$ for $\delta \to 0$). By having proved consistency and unconditional stability of the family of least squares semi-Lagrangian schemes, the Lax equivalence theorem ensures convergence of this numerical method.

2.2.1 Analysis

A contour plot of the amplification factors as a function of $\hat{\alpha}$ and δ is given in figures 2.2 and 2.3. The figures may be compared to the numerical dissipation in conventional semi-Lagrangian schemes outlined in figure 1 of [McDonald, 1984] (the α-axes on figure 1 in [McDonald, 1984] is not identical to the ones on figures 2.2(a) and 2.3(a)).

[2] a formal proof is part of the construction of the more general scheme (see chapter 3)
[3] details are given in Appendix A.3

$$
\begin{array}{rl}
\textbf{Linear} & \phi_I^{n+1} = \mathcal{A}_+^{(1)}\,\phi_{I-p-1}^n + \mathcal{B}^{(1)}\,\phi_{I-p}^n + \mathcal{A}_-^{(1)}\,\phi_{I-p+1}^n \\
\textbf{Quadratic} & \phi_I^{n+1} = \mathcal{A}_+^{(2)}\,\phi_{I-p-2}^n + \mathcal{B}_+^{(2)}\,\phi_{I-p-1}^n + \mathcal{B}_-^{(2)}\,\phi_{I-p}^n + \mathcal{A}_-^{(2)}\,\phi_{I-p+1}^n \\
\textbf{Cubic} & \phi_I^{n+1} = \mathcal{A}_+^{(3)}\,\phi_{I-p-2}^n + \mathcal{B}_+^{(3)}\,\phi_{I-p-1}^n + \mathcal{C}^{(3)}\,\phi_{I-p}^n + \mathcal{B}_-^{(3)}\,\phi_{I-p+1}^n + \mathcal{A}_-^{(3)}\,\phi_{I-p+2}^n \\
\textbf{Quartic} & \phi_I^{n+1} = \mathcal{A}\,\phi_{I-p-3}^n + \mathcal{B}_+^{(4)}\,\phi_{I-p-2}^n + \mathcal{C}_+^{(4)}\,\phi_{I-p-1}^n + \mathcal{C}_-^{(4)}\,\phi_{I-p}^n + \mathcal{B}_-^{(4)}\,\phi_{I-p+1}^n + \mathcal{A}_-^{(4)}\,\phi_{I-p+2}^n
\end{array}
$$

where the coefficients in the linear and quadratic cases are given by

$$
\begin{array}{ll}
\mathcal{A}_\pm^{(1)} = \frac{1}{3} \pm \frac{1}{2}\,\hat{\alpha} & \mathcal{A}_\pm^{(2)} = -\frac{1}{16} \pm \frac{3}{10}\,\hat{\alpha} + \frac{1}{4}\,\hat{\alpha}^2 \\
\mathcal{B}^{(1)} = \frac{1}{3} & \mathcal{B}_\pm^{(2)} = \frac{9}{16} \pm \frac{1}{10}\,\hat{\alpha} - \frac{1}{4}\,\hat{\alpha}^2
\end{array}
$$

For cubic and quartic fits the coefficients are given by

$$
\begin{array}{ll}
\mathcal{A}_\pm^{(3)} = -\frac{3}{35} \mp \frac{1}{12}\,\hat{\alpha} + \frac{1}{7}\,\hat{\alpha}^2 \pm \frac{1}{12}\,\hat{\alpha}^3 & \mathcal{A}_\pm^{(4)} = \frac{3}{256} \mp \frac{275}{3024}\,\hat{\alpha} - \frac{5}{96}\,\hat{\alpha}^2 \pm \frac{5}{108}\,\hat{\alpha}^3 + \frac{1}{48}\,\hat{\alpha}^4 \\
\mathcal{B}_\pm^{(3)} = \frac{12}{35} \pm \frac{2}{3}\,\hat{\alpha} - \frac{1}{14}\,\hat{\alpha}^2 \mp \frac{1}{6}\,\hat{\alpha}^3 & \mathcal{B}_\pm^{(4)} = -\frac{25}{256} \pm \frac{1249}{3024}\,\hat{\alpha} + \frac{13}{32}\,\hat{\alpha}^2 \mp \frac{7}{108}\,\hat{\alpha}^3 - \frac{1}{16}\,\hat{\alpha}^4 \\
\mathcal{C}^{(3)} = \frac{17}{35} - \frac{1}{7}\hat{\alpha}^2 & \mathcal{C}_\pm^{(4)} = \frac{75}{128} \pm \frac{163}{756}\,\hat{\alpha} - \frac{17}{48}\,\hat{\alpha}^2 \mp \frac{1}{27}\,\hat{\alpha}^3 + \frac{1}{24}\,\hat{\alpha}^4
\end{array}
$$

Table 2.1: Explicit formulas for up to fourth order accurate least squares schemes. ϕ_j^n is the numerical approximation to the true solution ψ at $(x,t) = (j\Delta, n\Delta t)$.

$$||\Gamma^{(1)}||^2 = 1 - c\left\{\left(\tfrac{4}{3} - 2\hat{\alpha}^2\right) + c\left(\hat{\alpha}^2 - \tfrac{4}{9}\right)\right\}$$

$$||\Gamma^{(2)}||^2 = 1 - c^2\left\{\left(-\hat{\alpha}^4 + \tfrac{19}{10}\hat{\alpha}^2 + \tfrac{3}{16}\right) + c\left(\tfrac{1}{2}\hat{\alpha}^4 - \tfrac{97}{100}\hat{\alpha}^2 + \tfrac{1}{32}\right)\right\}$$

$$||\Gamma^{(3)}||^2 = 1 - c^2\left\{\left(\tfrac{1}{3}\hat{\alpha}^4 - \tfrac{31}{21}\hat{\alpha}^2 + \tfrac{24}{35}\right) + c\left(-\tfrac{2}{9}\hat{\alpha}^6 + \tfrac{58}{63}\hat{\alpha}^4 - \tfrac{76}{315}\hat{\alpha}^2\right) + c^2\left(\tfrac{1}{9}\hat{\alpha}^6 - \tfrac{242}{441}\hat{\alpha}^4 + \tfrac{1109}{2205}\hat{\alpha}^2 - \tfrac{144}{1225}\right)\right\}$$

$$||\Gamma^{(4)}||^2 = 1 - c^3\left\{\left(\tfrac{1}{9}\hat{\alpha}^6 - \tfrac{95}{108}\hat{\alpha}^4 + \tfrac{3539}{3024}\hat{\alpha}^2 + \tfrac{5}{64}\right) + c\left(-\tfrac{1}{36}\hat{\alpha}^8 + \tfrac{71}{324}\hat{\alpha}^6 - \tfrac{5321}{18144}\hat{\alpha}^4 + \tfrac{53}{36288}\hat{\alpha}^2 + \tfrac{15}{1024}\right)\right.$$
$$\left. + c^2\left(\tfrac{1}{72}\hat{\alpha}^8 - \tfrac{805}{5832}\hat{\alpha}^6 + \tfrac{121453}{326592}\hat{\alpha}^4 - \tfrac{1388605}{4572288}\hat{\alpha}^2 + \tfrac{9}{2048}\right)\right\}$$

Table 2.2: Explicit formulas for the amplification factors for up to fourth order accurate least squares schemes. $\Gamma^{(1)}$ refers to the amplification factor of the scheme using a straight line fit, $\Gamma^{(2)}$ refers to Γ of the scheme using a parabola fit. $\Gamma^{(3)}$ and $\Gamma^{(4)}$ refers to Γ of the cubic and quartic schemes, respectively.

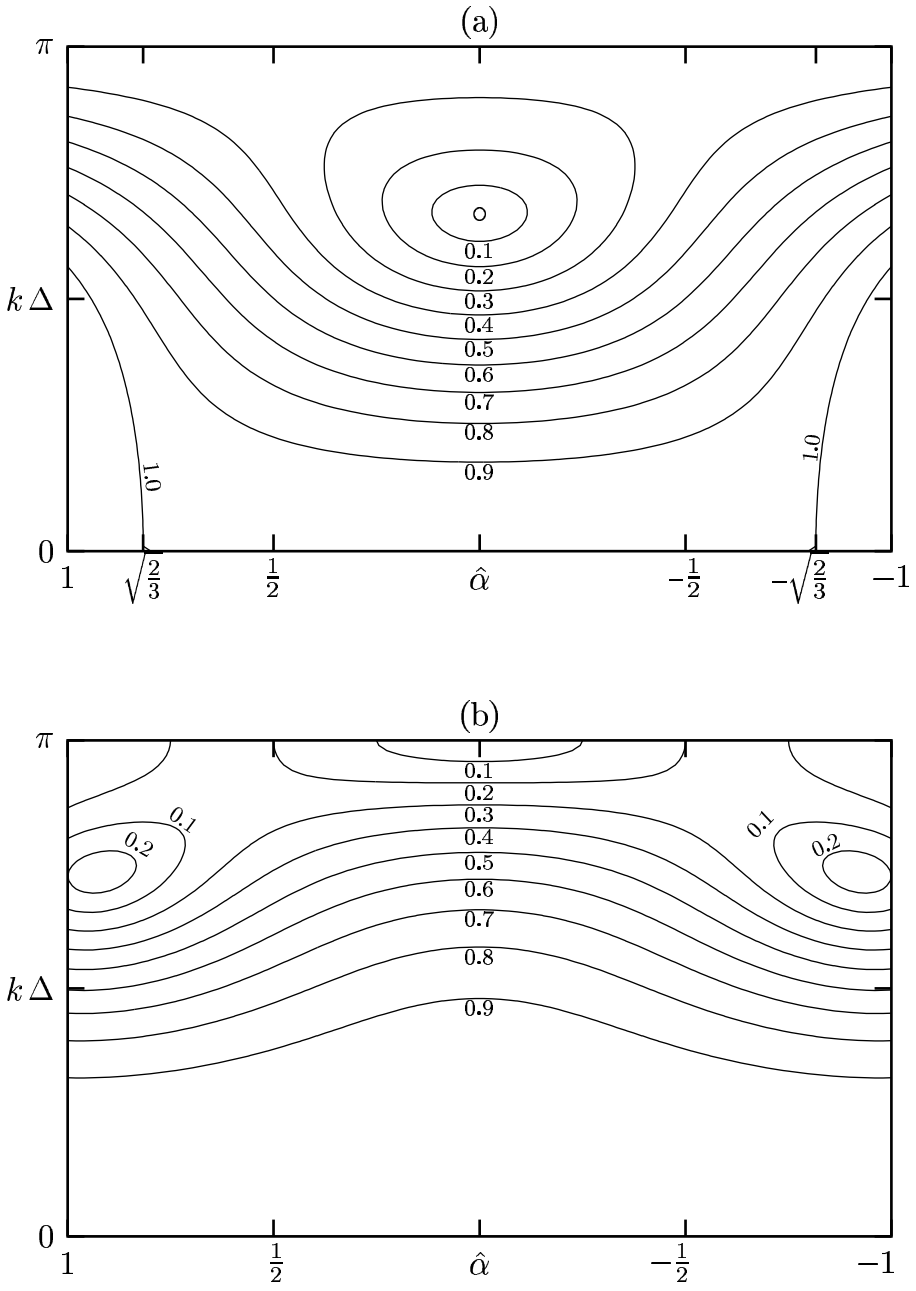

Figure 2.2: Isolines of the modulus of the amplification factor, $\|\Gamma\|$, as a function of $\hat{\alpha}$ and $k\,\Delta$ for (a) the linear and (b) the quadratic least squares schemes. The circle, $\circ$, marks the point where the linear scheme damp totally. Note that the amplification factor is plotted for $\hat{\alpha}$ exceeding the predefined $\hat{\alpha}$-interval (see equation (2.6)).

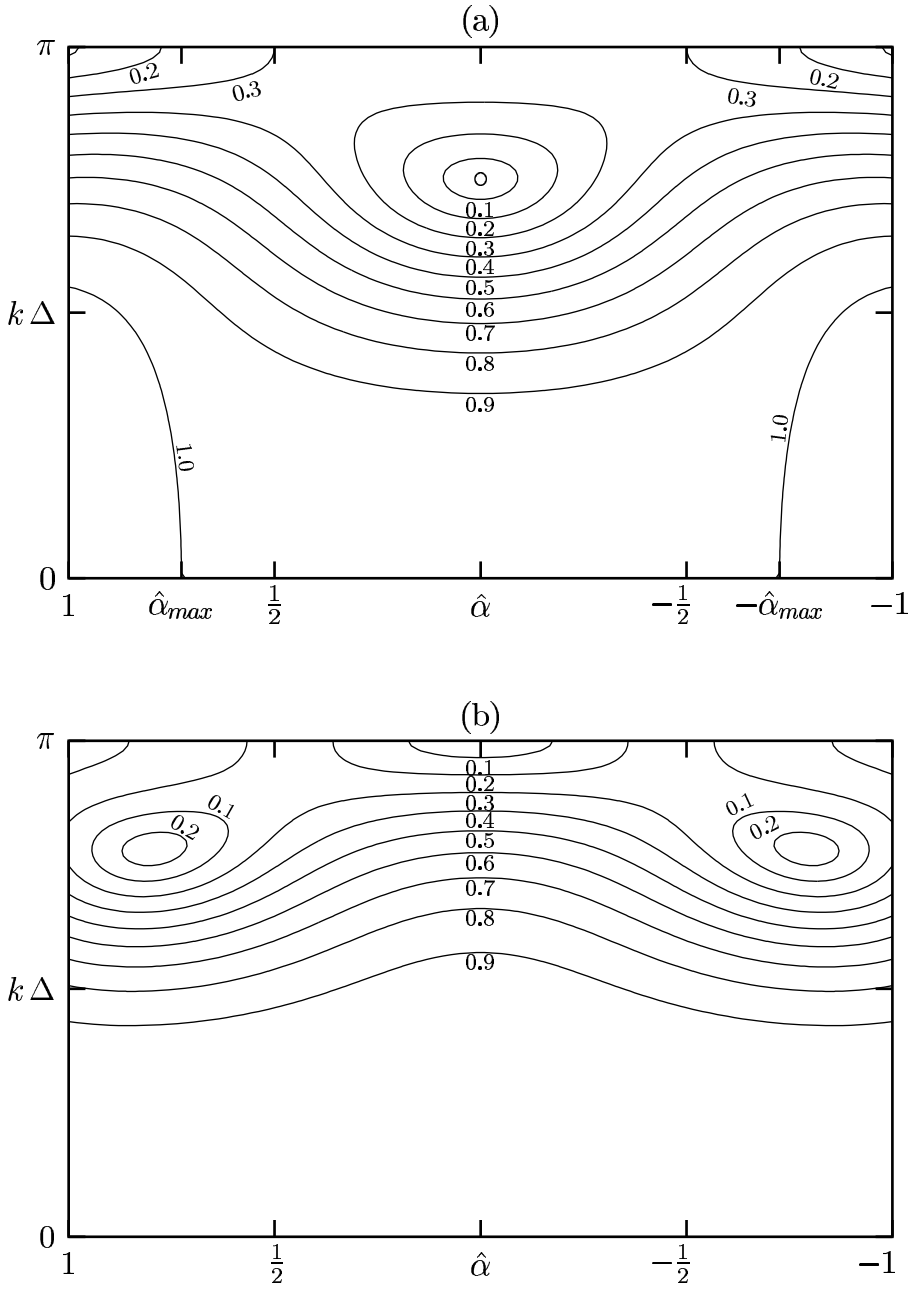

Figure 2.3: Same as figure 2.2, but for (a) the cubic and (b) the quartic least squares schemes. In (a) $\hat{\alpha}_{max}$ refers to the maximum unconditionally stable value of $\hat{\alpha}$.

Linear and cubic schemes The amplification properties of the linear and cubic schemes are quite similar. The amplification factors do not increase monotonically as a function of wavelength. In the linear case the 3Δ wave is damped completely for $\hat{\alpha} = 0$. The same happens when using the cubic scheme, but for the wavelength given by

$$\delta_c \equiv \cos^{-1}\left(1 - \tfrac{\sqrt{105}}{6}\right),$$

in terms of δ (corresponds to a wavelength of approximately 2.67Δ). Having exceeded the wavelength of maximum damping the dissipation decreases monotonically towards neutral damping.

Figures 2.2(a) and 2.3(a) indicate that the schemes are stable even for $|\hat{\alpha}|$ values exceeding $\frac{1}{2}$. The linear scheme is unconditionally stable for $|\hat{\alpha}|$ as large as $\sqrt{\frac{2}{3}}$. The amplification factor actually improves for $|\hat{\alpha}| > \frac{1}{2}$. When considering only amplification properties, the original choice of p in equation (2.2), which was chosen for symmetry reasons, seems not to be an optimal choice. In order to improve dissipation properties of the scheme, one could shift the interval by the amount: $\sqrt{\frac{2}{3}} - \frac{1}{2}$.

The cubic case is similar to the linear one. $|\hat{\alpha}|$ can take values as large as $\hat{\alpha}_{max}$, given by[4]

$$\alpha_{max} \equiv \tfrac{1}{70}\sqrt{10850 - 70\sqrt{13945}},$$

without changing unconditional stability. When exceeding $|\hat{\alpha}| = \frac{1}{2}$, the amplification factor improves, apart from very short wavelengths (less than $\frac{5}{2}\Delta$). Again, one could simply shift the $\hat{\alpha}$-interval to improve dissipation properties. However, note that in both cases a shift in the $\hat{\alpha}$-interval will not remove the regions of poorest amplification properties ($\hat{\alpha} \approx 0$).

Quadratic and quartic schemes Figures 2.2(b) and 2.3(b) reveal that the choice of p given by equation (2.3) gives a better amplitude representation than if, for instance, p had been chosen by equation (2.2). Contrary to the linear and cubic schemes, only very small wavelengths (less than 3Δ) would benefit from such a shift.

For given $\hat{\alpha}$, the damping decreases for increasing wavelength. In other words, $||\Gamma||$

[4] $\alpha_{max} \approx 0.726$

is a monotonic function of δ. Compared to conventional semi-Lagrangian schemes, the damping is quite uniform with respect to varying $\hat{\alpha}$ values. Unless the wavelength is very short (less than 3Δ) the amplitude representation is best when the departure point is located in the center of the fitting interval ($\hat{\alpha} = 0$). This stands in contrast to conventional semi-Lagrangian schemes, which have the poorest amplitude representation when the departure point is located midway between grid points.

2.3 Relative phase speed

Another calculable measure of the quality of a scheme is its ability to represent the correct phase-speed. Write the numerical amplification factor in the form

$$\Gamma = ||\Gamma|| \exp\left(-i\omega^* \Delta t\right),$$

where $||\Gamma||$ is given in section 2.2. By basic algebra with complex numbers we have

$$\omega^* \Delta t = p\, k\, \Delta - \arctan\left(\frac{\Im\{\Gamma \cdot e^{i\, pk\Delta}\}}{\Re\{\Gamma \cdot e^{i\, pk\Delta}\}}\right). \tag{2.7}$$

The real and imaginary part of $\Gamma \cdot e^{i\, pk\Delta}$ may easily be computed from the expressions given in appendix A.3. It is useful to characterize the phase error through the relative phase change, R, which is defined as

$$R \equiv \frac{\omega^*}{\omega}, \tag{2.8}$$

where ω is the analytical frequency given by kU. In terms of p and $\hat{\alpha}$, the wind speed U can be written as

$$U = \Delta \cdot \begin{cases} (p + \hat{\alpha}) & N \text{ odd} \\ \left(p + \hat{\alpha} + \frac{1}{2}\right) & N \text{ even.} \end{cases} \tag{2.9}$$

By using equations (2.7), (2.8) and (2.9), one can write down the explicit formulas for the relative phase-speed error as a function of $\hat{\alpha}$ and p.

2.3.1 Analysis

A contour plot of R as a function of wavelength and distance between the x value of the departure point and the x value of the arrival point is given in figures 2.4 and 2.5. These figures may directly be compared to figure 2 of [McDonald, 1984], if a comparison to conventional semi-Lagrangian schemes is desired[5]. As for conventional semi-Lagrangian schemes, the phase representation improves as advection becomes more and more dominant (p increasing). For fixed $\hat{\alpha}$ the phase errors decrease as the wavelength increases (for linear and cubic schemes this is only correct if we require the wavelength to be longer than the for $\hat{\alpha} = 0$ completely damped one).

Linear and cubic schemes A first glance at the contour plot of figures 2.4(a) and 2.5(a) unveils rather complicated behavior at short wavelengths. When the departure point coincides with grid points, it was observed in section 2.2 that for a certain wavelength the schemes were completely damping. At this $(\hat{\alpha}, \delta)$-point, ω^* is not defined as $\Re\{\Gamma\}$ is zero, while $\Im\{\Gamma\}$ is non-zero. In other words, this $(\hat{\alpha}, \delta)$-point defines a singular point for R. When the departure point is in the neighborhood of grid points and the wavelength is close to the for $\hat{\alpha} = 0$ completely damped one, the relative phase change has strong gradients.

When the departure point coincides with grid points, the phase-speed representation is exact but the damping is maximal. When U is small ($p = 0$ and $\hat{\alpha}$ small) and the wavelength is less than or equal to the for $\hat{\alpha} = 0$ completely damped one, the finite difference schemes become extremely accelerating.

It was noted in section 2.2.1 that these schemes were unconditionally stable and less damping for $|\hat{\alpha}|$ values exceeding $\frac{1}{2}$. The question is whether the phase-error improves as well ? Figures 2.6 and 2.7 show the phase representation when $|\hat{\alpha}|$ exceeds $\frac{1}{2}$ for p equal to 0 and 1. Comparing to the original choice of p given in figures 2.4 and 2.5, the phase representation improves as well when going to larger $\hat{\alpha}$ values. Considering both amplitude and phase errors, we may conclude that the choice of p given in (2.2) is not an optimal choice. The scheme would improve both

[5] although the notation on the x-axises on the figures of this study and figure 2 in [McDonald, 1984] differ, the axises are in fact identical

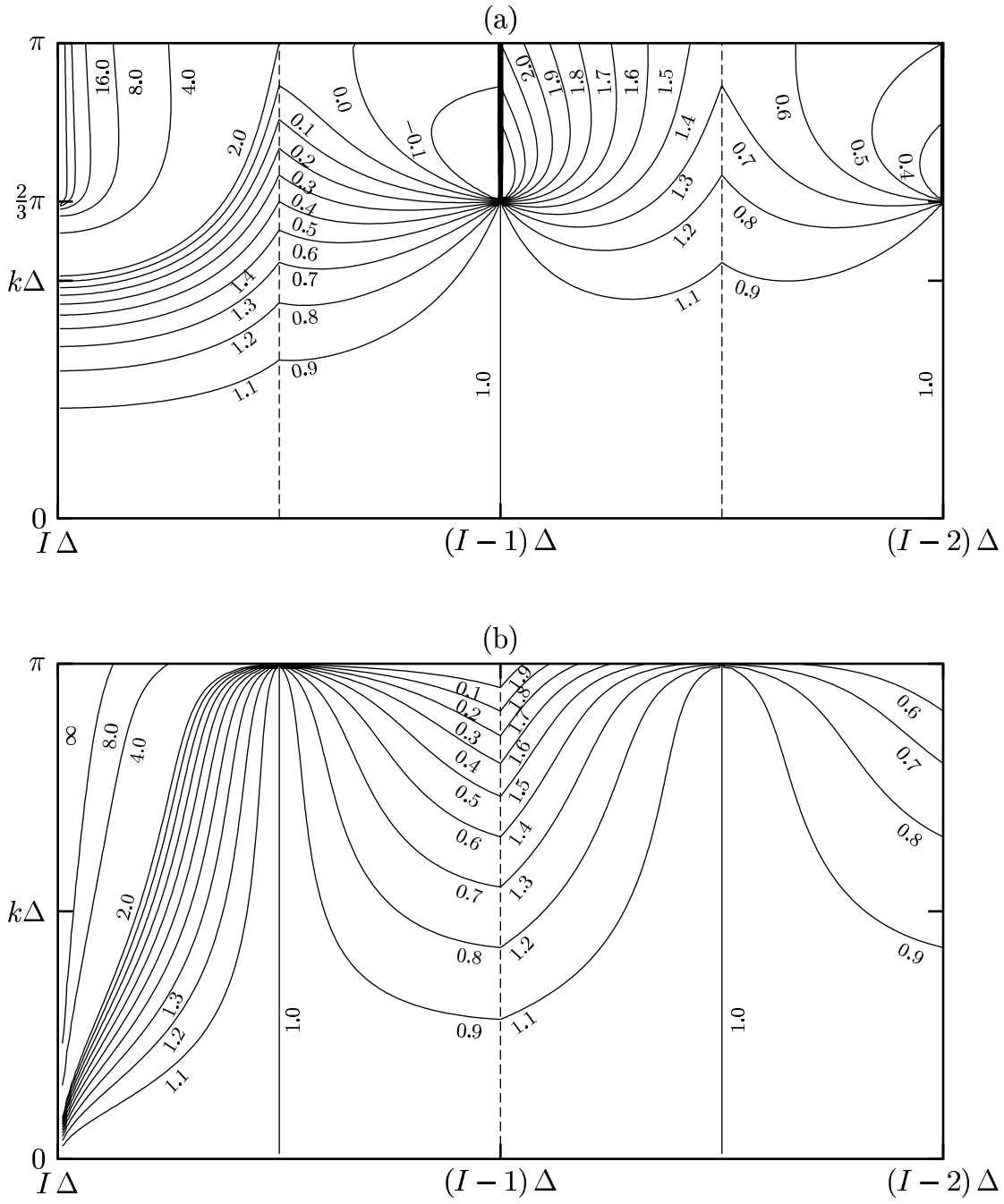

Figure 2.4: Isolines of the relative phase change, R, plotted as a function of $k\,\Delta$ and departure point for (a) the linear and (b) the quadratic least squares schemes.

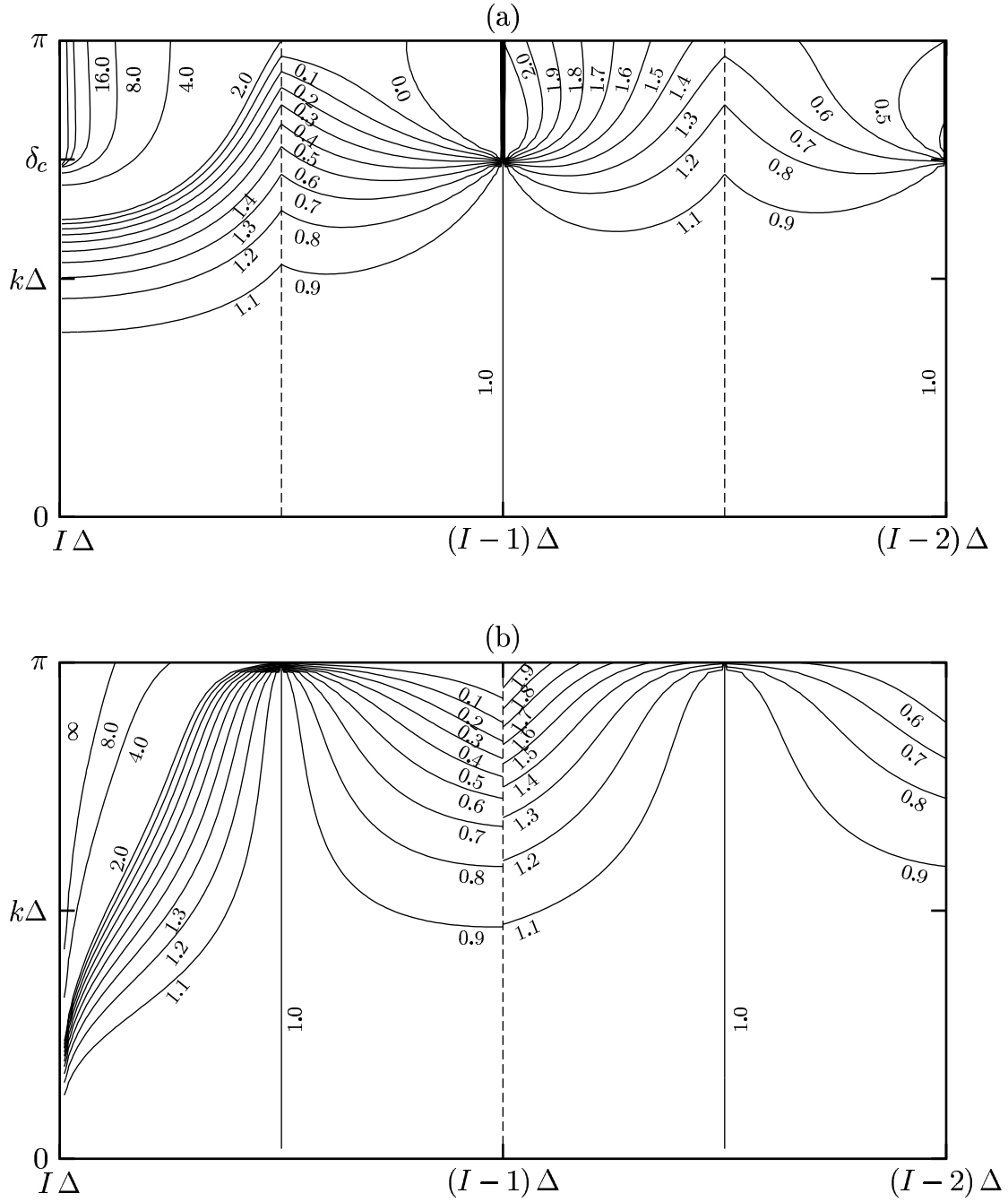

Figure 2.5: Same as figure 2.4, but for (*a*) the cubic scheme and (*b*) the quartic scheme.

amplitude and phase representation by a simple shift of the $\hat{\alpha}$-interval. However, the regions of poorest amplitude and phase properties are not eliminated by performing a shift in the $\hat{\alpha}$-interval.

Quadratic and quartic schemes For these schemes there is no wavelength which is completely damped, and R does not have singular points. By keeping $\hat{\alpha}$ fixed, the phase representation improves as the wavelength increases. Again, we can notice an extreme acceleration when U approaches zero. This time the acceleration covers nearly the entire range of wavelengths. An interesting fact is that the phase representation is exact midway between grid points. So the damping is least and phase representation exact when the departure point is furthest away from grid points, $\hat{\alpha} = 0$.

Ordering the schemes according to ability to represent phase is highly dependent on where the departure point is located. It is not obvious which scheme is superior. The odd-order schemes are preferable when the departure point is near grid points and the even-order schemes are most faithful in between grid points. Performing the above mentioned shift to the odd-order schemes would add more regions of little phase-error in between grid points. It was also noticed that all schemes are quite accelerating when U is little. The odd-order schemes, however, only demonstrate this property for short wavelengths.

2.4 Possible improvements

Summing up amplitude and phase properties of the family of least squares schemes, we must conclude that this approach does not provide any significant advantages in terms of stability. However, in order to make a complete analysis of a numerical advection scheme, one has to evaluate many other properties [Rasch and Williamson, 1990]. Rather than continuing the investigation of properties restricted to the family of least squares schemes, a more general approach is taken. The generalization was triggered by the poor results obtained and the subsequent question of whether improvements within the least squares framework are possible or not. Answering this question

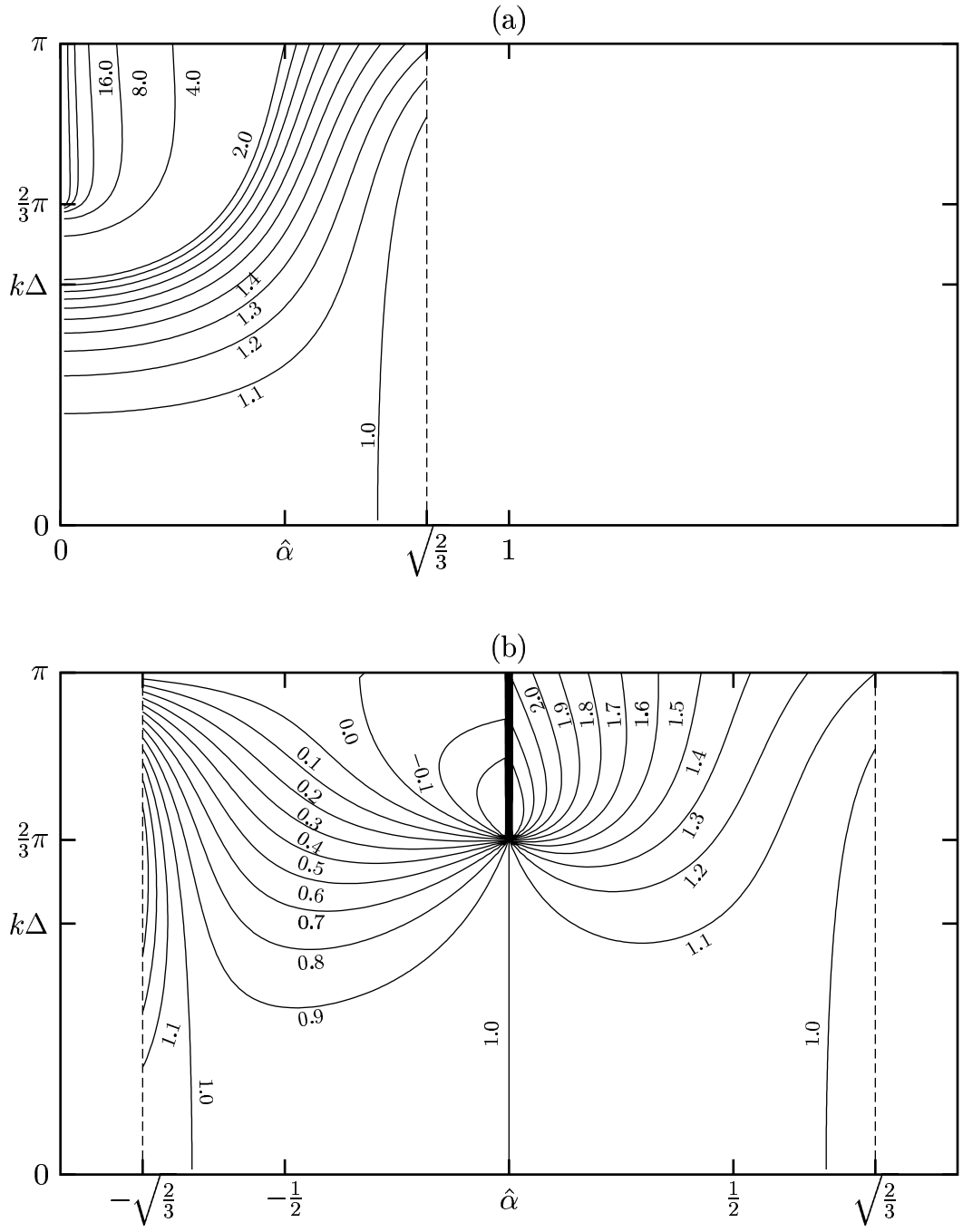

Figure 2.6: Isolines of R as a function of $\hat{\alpha}$ and δ for the linear scheme for (a) $p = 0$, (b) $p = 1$. For comparison, the $\hat{\alpha}$-axes is identical to the grid point axes of figure 2.2.

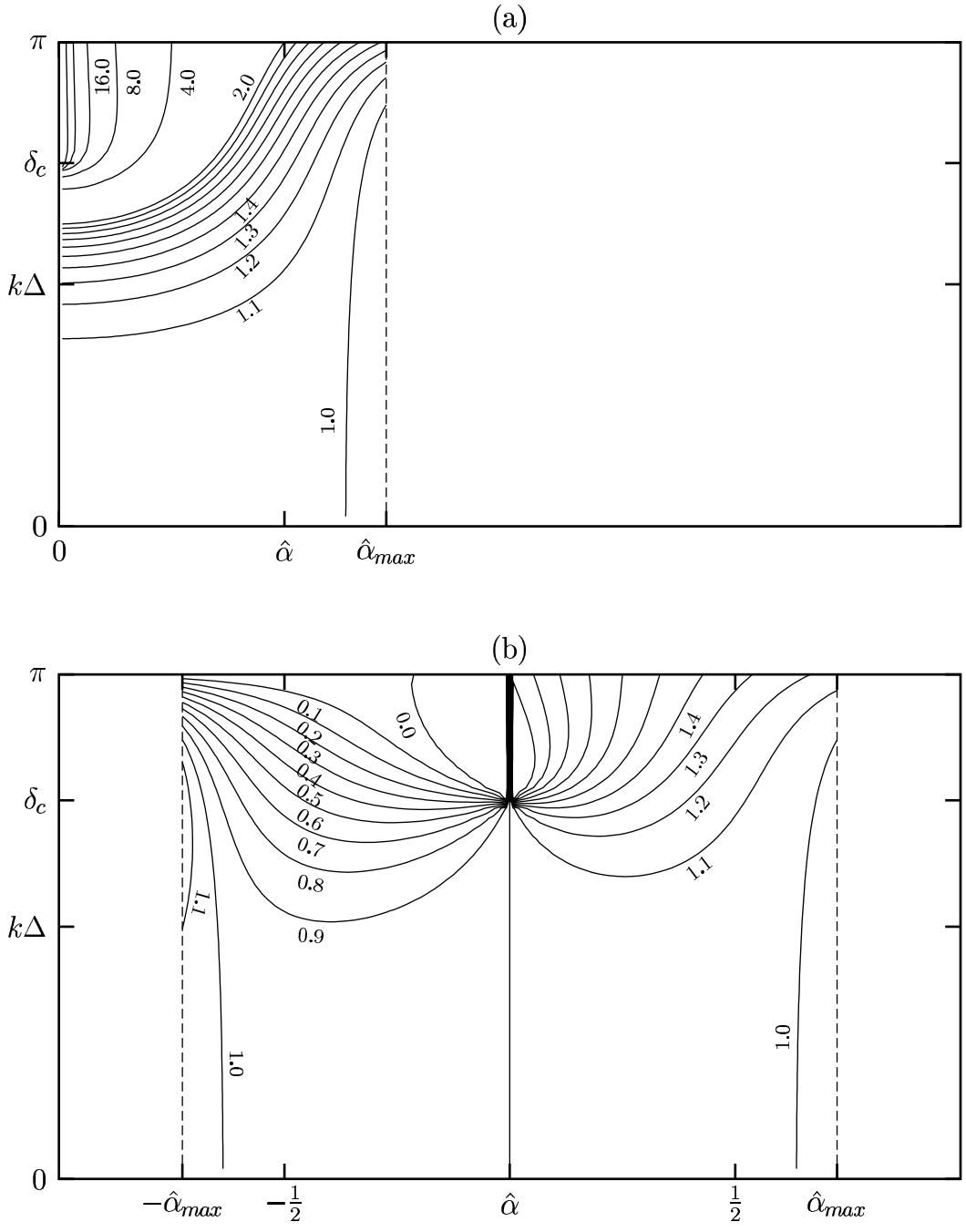

Figure 2.7: Same as figure 2.6, but for the cubic scheme.

may be used to motivate a more general analysis as demonstrated in the coming paragraphs.

It might be argued that the least squares approach violates the principle of locality. Near a grid point the least squares method weights all points equal. Consequently, distant grid point values have as much influence as nearby grid point values. This causes excessive damping at short wavelengths and prevents the scheme from being exact when departure points coincide with grid points.

One way to improve the locality property is to make a, in principle, simple modification to the least squares method by introducing weighted least squares[6]. For example, the weighted linear least squares scheme given by

$$\phi_I^{n+1} = \left(\frac{2\,(1+\hat{\alpha})\,{\sigma_2}^2 + \hat{\alpha}\,{\sigma_3}^2}{{\sigma_1}^2 + 4\,{\sigma_2}^2 + {\sigma_3}^2}\right)\phi_{I-p-1}^n + \left(\frac{(1+\hat{\alpha})\,{\sigma_1}^2 + (1-\hat{\alpha})\,{\sigma_3}^2}{{\sigma_1}^2 + 4\,{\sigma_2}^2 + {\sigma_3}^2}\right)\phi_{I-p}^n + \left(\frac{2\,(1-\hat{\alpha})\,{\sigma_2}^2 - \hat{\alpha}\,{\sigma_1}^2}{{\sigma_1}^2 + 4\,{\sigma_2}^2 + {\sigma_3}^2}\right)\phi_{I-p+1}^n ,$$

where $\frac{1}{\sigma_i^2}$ $(i = 1, 2, 3)$ are weighting functions. By applying this method, the influence of distant grid point values can be reduced. The fit can even be made exact at grid points if desired ($\sigma_2 = 0$). However, introducing weighted least squares also introduces a non-obvious choice of weighting functions. Apart from general intuitive guidelines, such as choosing distance dependent weighting functions ($\sigma_i = \sigma_i(\hat{\alpha})$), there seems to be no straightforward way of constructing them. Relying solely on intuition might be misleading. Instead of using a brute force method of simply trying out different weighting functions one might try to take a more constructive approach. Based on Taylor series expansions, we will derive a class of schemes which permit comparison of possible convergent weighted least squares schemes, without explicit construction and brute force testing of various "random" weighting functions. Investigating properties of the latter class of schemes provides insights which are very useful when trying to construct a feasible interpolation method for semi-Lagrangian schemes.

[6] see A.2.4

Chapter 3

A more General Scheme

Notation The same notation as introduced in chapter 2 will be used, except for the definition of the interpolary parameter $\hat{\alpha}$ given by equation (2.5). The former definition was chosen in order to introduce symmetry in derived formulas and simplify computations. In this context it will simplify notation not to let $\hat{\alpha}$ depend on whether the number of grid point values used during the interpolation, N, is even or odd. Therefore redefine equation (2.5)

$$\hat{\alpha} \equiv \alpha - p\,.$$

Note that the change in notation implies that (2.6) is no longer valid for N even, in which case we have

$$0 \leq \hat{\alpha} < 1\,. \tag{3.1}$$

In addition define

$$N^- \equiv \begin{cases} -\frac{N}{2} & N \text{ even} \\ -\left[\frac{N}{2}\right] & N \text{ odd,} \end{cases} \qquad N^+ \equiv \begin{cases} \frac{N}{2} - 1 & N \text{ even} \\ \left[\frac{N}{2}\right] & N \text{ odd,} \end{cases} \tag{3.2}$$

where $[\cdot]$ is the smallest integer less than or equal to the argument.

Again, consider the one-dimensional advection equation (2.1) and let it be defined

on a periodic domain $\mathcal{D}$, which is discretized using M equidistant increments of Δ.

3.1 Consistent schemes

In general, a semi-Lagrangian scheme using N points for interpolation can be written in the form

$$\phi_I^{n+1} = A_1\phi^n_{(I-p+N^-)} + A_2\phi^n_{(I-p+N^-+1)} + ... + A_{N-1}\phi^n_{(I-p+N^+-1)} + A_N\phi^n_{(I-p+N^+)}\,. \tag{3.3}$$

The functions $A_1, A_2, ..., A_{N-1}$ and A_N are to be chosen. In general, A_i is a function of $\hat{\alpha}$ and grid point values $\phi^n_{I-p+N^-}$, $\phi^n_{I-p+N^-+1}$, ...,$\phi^n_{I-p+N^+}$. Conventional schemes using Lagrange interpolation, as well as the least squares method, use A_i's which are only functions of the interpolation parameter $\hat{\alpha}$ and do not depend on the specific distribution. The same is the case for a weighted least squares scheme using weight functions which depend only on $\hat{\alpha}$. If the A_i's are functions of grid point values, the scheme becomes non-linear, which complicates the analysis. An example of a scheme using distribution dependent A_i's is one which uses Hermite interpolation. Note that a scheme using spline interpolation is not[1] a scheme on the form (3.3). A spline interpolant is a global interpolation method contrary to local ones which only use a fixed number of neighboring grid point values. Clearly (3.3) defines a local interpolant.

To facilitate the coming analysis consider distribution independent choices of the A_i's unless else is explicitly stated. Thereby we formally exclude Hermite type schemes from the coming analysis and narrow the discussion to schemes using local interpolators.

[1] unless $N = M$

3.1.1 Truncation error

Substitution of Taylor series expansions about the departure point, (x_*, t^n), into the general finite difference formula (3.3), yields the truncation error

$$(3.4)\quad (1 - A_1 - A_2 - ... - A_N)\,\frac{\psi_d}{\Delta t} - \sum_{m=1}^{\infty} \frac{1}{m!}\left[A_1\left(\hat{\alpha} + N^-\right)^m + A_2\left(\hat{\alpha} + N^- + 1\right)^m + ... + A_N\left(\hat{\alpha} + N^+\right)^m\right] \left.\frac{\partial^m \psi}{\partial x^m}\right|_d \frac{\Delta^m}{\Delta t},$$

where $\psi_d = \psi(x_*, n\Delta t)$. Obviously a necessary condition for consistency is that

$$(3.5)\qquad A_1 + A_2 + A_3 + ... + A_N = 1\,.$$

Furthermore, inspection of the first term in the sum reveals that a second necessary condition for consistency is that this term vanishes as well, i.e.

$$(3.6)\quad A_1\left(\hat{\alpha} + N^-\right) + A_2\left(\hat{\alpha} + N^- + 1\right) + ... + A_{N-1}\left(\hat{\alpha} + N^+ - 1\right) + A_N\left(\hat{\alpha} + N^+\right) = 0.$$

These two conditions guarantee that the scheme will be consistent and at least of order $\mathcal{O}\left(\Delta t, \Delta, \frac{\Delta^2}{\Delta t}\right)$. Note that, in general, we must require the Courant number to be held constant when performing the limit $\Delta t, \Delta \to 0$. Higher order formal accuracy, say kth-order, is obtained by fulfilling (3.5), (3.6) and by assuring that all terms in the sum (3.3) from $m = 2$ to $m = k - 1$ vanish. The A_i's yielding maximum order of accuracy are calculated by solving the system

$$\begin{aligned}
A_1 + A_2 + A_3 + ... + A_N - 1 &= 0\,,\\
A_1\left(\hat{\alpha} + N^-\right) + ... + A_N\left(\hat{\alpha} + N^+\right) &= 0\,,\\
A_1\left(\hat{\alpha} + N^-\right)^2 + ... + A_N\left(\hat{\alpha} + N^+\right)^2 &= 0\,,\\
\vdots \qquad\qquad\qquad \vdots &\qquad \vdots\\
A_1\left(\hat{\alpha} + N^-\right)^{N-1} + ... + A_N\left(\hat{\alpha} + N^+\right)^{N-1} &= 0\,,
\end{aligned}$$

of N equations for N unknowns. Consequently, the coefficients, A_1, ..., A_{N-1} and A_N are uniquely determined and can easily be shown to be equal to the coefficients of the $(N-1)$th-order conventional Lagrange interpolator. It is evident that seeking even higher order accuracy will result in having to solve an overdetermined system of equations, which in general does not have any solution. Hence the highest possible order of accuracy is $(N-1)$th-order.

Given the number of grid points one wishes to use for the interpolation, conventional Lagrange interpolation is optimal in terms of formal accuracy. High order of spatial accuracy is, of course, a much desired property. However, in the vicinity of discontinuities or shocks the former analysis based on Taylor series expansions is rather useless. Increasing accuracy may even be counterproductive in the vicinity of abrupt changes in the field ψ. Other important information not revealed by an accuracy analysis is information about concepts like monotonicity and conservation. These are among many properties which are important to consider when trying to construct a feasible scheme for modeling of geophysical flows.

Relaxing one order of the maximum obtainable accuracy creates one degree of freedom. The idea is to exploit this degree of freedom in order to try and enforce desirable properties. The least squares interpolation method is of $(N-2)$th-order, i.e. one order less than the maximum obtainable order of formal accuracy. The scheme did not improve amplitude or phase properties. However, it will be shown shortly, that the least squares scheme is only one among many convergent $(N-2)$th-order schemes on the form given by equation(3.3).

For simplicity let N be equal to three. The results are, however, in general characteristic of equivalent higher order schemes using more points during the interpolation process.

3.2 General three point schemes

Solving the two consistency equations, equations (3.5) and (3.6), for A_2 and A_3 yields

$$\begin{aligned} A_2 &= 1 + \hat{\alpha} - 2A_1 \,, \\ A_3 &= A_1 - \hat{\alpha} \,. \end{aligned} \tag{3.7}$$

Hence consistent three point schemes are on the form

$$\phi_I^{(n+1)} = A_1 \, \phi_{I-p-1}^n + (1 + \hat{\alpha} - 2A_1) \, \phi_{I-p}^n + (A_1 - \hat{\alpha}) \, \phi_{I-p+1}^n \,, \tag{3.8}$$

where A_1 is the free parameter. Note that varying A_1 may be regarded as an analysis of the possibilities in introducing weighted least squares, since by proper choice of A_1 any linear and consistent three point semi-Lagrangian scheme can be written on the form (3.8). For example choosing A_1 equal to $\hat{\alpha}$ in (3.8) yields the conventional first order semi-Lagrangian scheme[2], A_1 equal to $\frac{1}{2}\hat{\alpha}(1 + \hat{\alpha})$ results in the conventional quadratic semi-Lagrangian scheme and A_1 equal to $\frac{1}{2} + \frac{1}{3}\hat{\alpha}$ yields the linear least squares scheme. As will be shown shortly, these are only three out of many convergent schemes on the form (3.8). Instead of constructing rather "random" weighting functions, which might result in unstable schemes, the "free parameter" approach seems more constructive.

3.2.1 Stability analysis

Performing a Von Neumann analysis yields the amplification factor and relative phase speed. Performing the substitutions outlined in sections 2.2 and 2.3 yields the squared modulus of the amplification factor

$$||\Gamma||^2 = 1 - 2c \left(2A_1 - \hat{\alpha} - \hat{\alpha}^2\right) - 4A_1 c^2 \, (\hat{\alpha} - A_1) \,, \tag{3.9}$$

[2]only if $\hat{\alpha} \geq 0$, otherwise the central grid point,x_{I-p}, does not correspond to the one of the conventional semi-Lagrangian scheme

and the relative phase speed

$$R = \frac{1}{\delta\,(\hat{\alpha}+p)}\left\{\delta\,p + \arctan\left(\frac{\hat{\alpha}\,\sin\delta}{1-(1-\cos\delta)\,(2A_1-\hat{\alpha})}\right)\right\},$$

where $\delta \equiv k\,\Delta$ and $c \equiv 1-\cos\delta$.

Amplification factor of convergent schemes

To guarantee the highly desirable property, unconditional stability, the following lemma imposes bounds on the values which A_1 may take. The proof is given in appendix A.4.

Lemma 1 *A consistent three point scheme is unconditionally stable if and only if* A_1 *is in the interval given by*

$$\left[A^-, A^+\right] \equiv \left[\tfrac{1}{2}\hat{\alpha}(1+\hat{\alpha}), \tfrac{1}{2}(1+\hat{\alpha})\right].$$

We will refer to A^+ and A^- as the maximum and minimum unconditional stable value of A_1, respectively[3]. As a consequence of Lax's theorem, the family of schemes on the form (3.8) are convergent when A_1 is in the above interval. The squared modulus of the amplification factor is plotted in figure 3.1 as a function of wavelength and the free parameter A_1 for selected $\hat{\alpha}$ values. Note that the A_1 value corresponding to the conventional quadratic Lagrange interpolation yields overall optimal amplitude properties. This is true for all valid $\hat{\alpha}$ values. Hence, the three point scheme with highest possible formal accuracy has superior amplification properties. It will, however, be demonstrated later that this is not always the case for schemes using more points during the interpolation process. Figure 3.1 also shows that there exists no A_1 value for which all wavelengths are non-damped or equally damped.

[3]the notation A^- and A^+ has nothing to do with N^- and N^+ defined on page 25

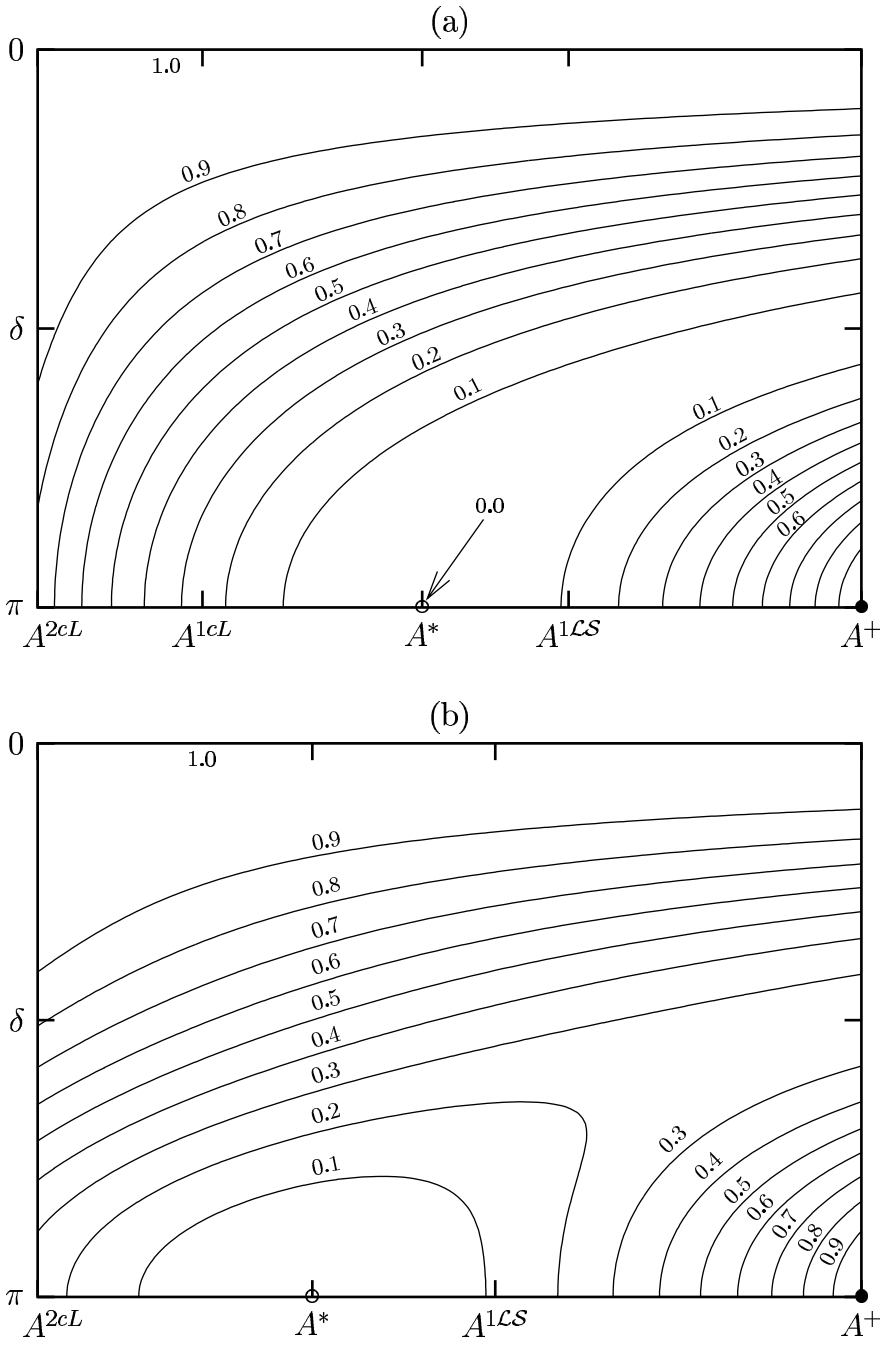

Figure 3.1: Isolines of the squared modulus of the amplification factor plotted as a function of A_1 and δ for (a) $\hat{\alpha} = \frac{1}{4}$ and (b) $\hat{\alpha} = -\frac{1}{2}$. The circles/(bullets), $\circ/(\bullet)$, mark the points where the scheme is completely/(neutrally) damping. A^* is explained in section 3.2.1. $A^{1\mathcal{LS}}/(A^{1cL})$ denote the A_1 value resulting in the linear least squares scheme/(first order conventional semi-Lagrangian scheme). Similarly, A^{2cL} is the A_1 value for which the scheme equals the conventional quadratic semi-Lagrangian scheme. Note that A^{2cL} is equal to A^-.

Relative phase speed of convergent schemes

Optimizing the relative phase speed, R, with respect to A_1 is less obvious than optimizing the amplification factor. We do not have a requirement of keeping R less than some value as was the case when considering amplification. However, we have restrictions on A_1 from the amplification analysis. An additional complication is that R is a function of $(A_1, \hat{\alpha}, \delta, p)$. Therefore visualization including all parameters is impossible. From experience with conventional semi-Lagrangian schemes as well as the least squares schemes, the phase speed properties improve when advection gets more and more dominating (p increasing). Therefore in most of the coming analysis we consider only the expected worst case of $p = 0$. By keeping either $\hat{\alpha}$ or δ fixed we can make contour plots of R and analyze the tendencies at different A_1 values.

2Δ wave Begin the analysis by considering the shortest resolvable wavelength ($\delta = \pi$). For that wavelength R reduces to

$$R = \frac{\pi\, p + \frac{1}{2}\pi\, \{1 - \mathrm{sgn}(1 - 4\, A_1 + 2\, \hat{\alpha})\}}{\pi\, (p + \hat{\alpha})}\,,$$

where sgn() denotes the signum function which equals 1 if the argument is positive and -1 if the argument is negative. For fixed p and $\hat{\alpha}$ values there is a discontinuous jump at the A_1 value, A^*, given by[4]

$$A^* \equiv \tfrac{1}{4} + \tfrac{1}{2}\hat{\alpha}\,,$$

between two constant values

$$R\big|_{L=2\Delta} = \begin{cases} R^+ & \text{for } A_1 > A^* \\ R^- & \text{for } A_1 < A^*\,, \end{cases}$$

[4]note that $A_1 = A^*$ also marks the point where the 2Δ wave is completely damped (see figure 3.1)

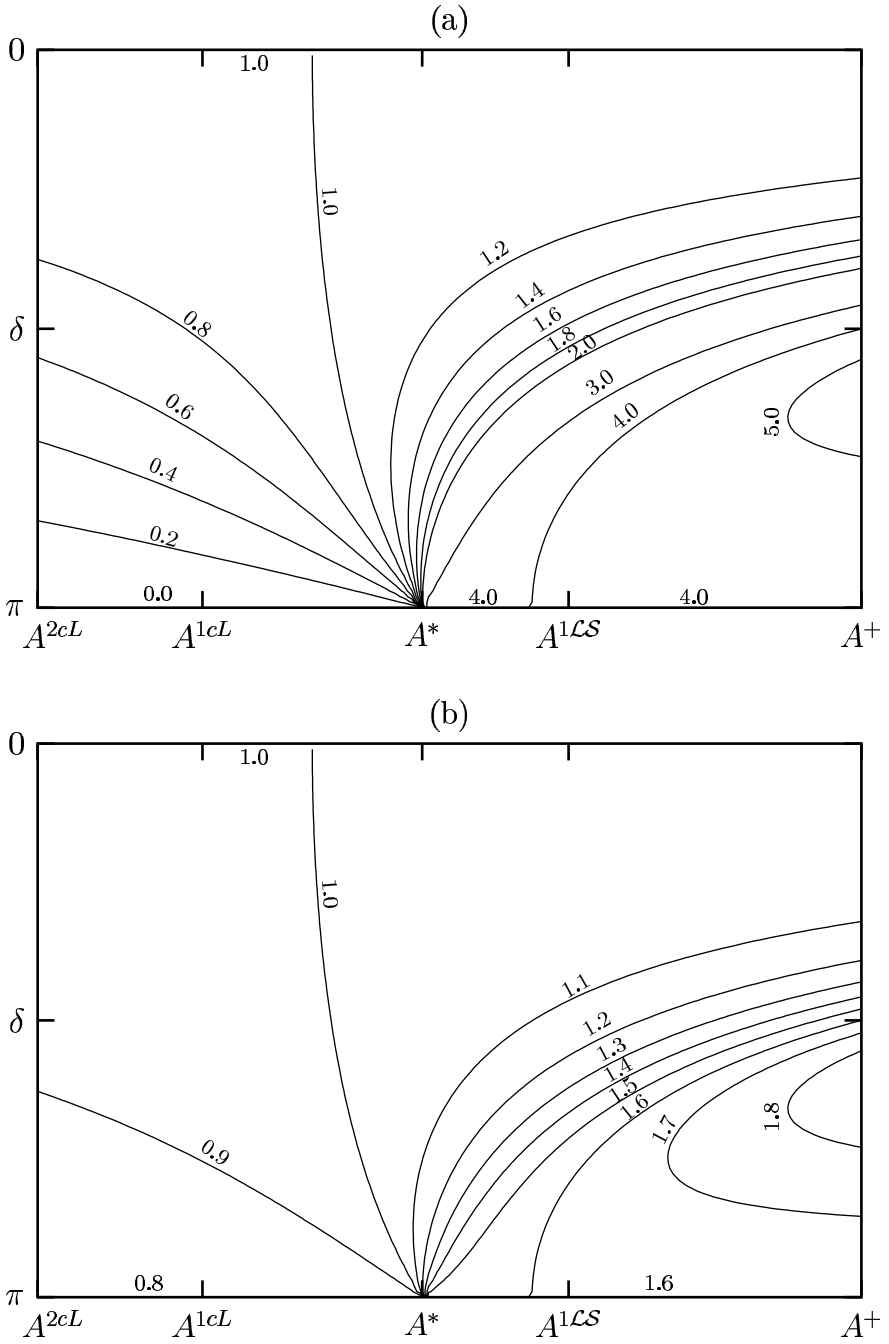

Figure 3.2: Isolines of the relative phase speed R for $\hat{\alpha} = \frac{1}{4}$ are plotted as a function of (A_1, δ) for (a) $p = 0$ and (b) $p = 1$. Notation is equivalent to figure 3.1. Note that A^* marks the abrupt change in R at short wavelengths, as well as the A_1 value for which the $2\,\Delta$ wave is completely damped. Its value is given by equation (3.12).

where

$$R^- \equiv \frac{p}{p+\hat{\alpha}} \qquad \text{and} \qquad R^+ \equiv \frac{p+\text{sgn}(\hat{\alpha})}{p+\hat{\alpha}}\,. \tag{3.10}$$

Note that increasing the p value reduces the discontinuous jump. In the special case of p equal to zero $R^\pm$ reduce to

$$R^- = 0 \qquad \text{and} \qquad R^+ = \frac{1}{\hat{\alpha}}\,. \tag{3.11}$$

Consequently, $R^+ \to \infty$ for $\hat{\alpha} \to 0$, which is an unfortunate property. For arbitrary p values we have

$$||R^- - 1|| \leq ||R^+ - 1|| \Leftrightarrow |\hat{\alpha}| \leq |\text{sgn}(\hat{\alpha}) - \hat{\alpha}|\,,$$

which demonstrates[5] that, except for $\hat{\alpha} = -\frac{1}{2}$, R^- is always closer to 1 than R^+.

So in terms of phase properties of the 2Δ wave it is preferable to choose A_1 such that

$$A_1 < A^*\,. \tag{3.12}$$

Constant interpolary parameter, $\hat{\alpha} = \frac{1}{4}$ Now keep $\hat{\alpha}$ constant at the representative value of $\frac{1}{4}$. Figure 3.2 shows that not only for the 2Δ wave, but for all short wavelengths, fulfilling (3.12) results in superior phase representation. The overall optimal choice of A_1 in terms of phase speed seems to be in the vicinity of A^* (see figure 3.2), which is very close to the overall worst amplitude representation, $A_1 = A^*$.

This is yet another demonstration of the tedious reality often encountered when working with numerical advection algorithms: Improvement of one property comes with the magnification of the error of another property. In this case an improvement in phase properties will worsen the overall amplitude representation and vice versa. It is not clear how phase and amplitude error should be weighted when choosing an optimum value of A_1. Nevertheless, in this simple case any choice of A_1 will

[5] using that $-\frac{1}{2} \leq \hat{\alpha} < \frac{1}{2}$

produce a scheme with a numerical diffusion too high for any practical use. Advantages are, however, not negligible when using first order methods selectively in the vicinity of shocks or discontinuities [Bermejo and Staniforth, 1992]. First order methods can also be used in a post adjustment algorithm to insure conservation of mass [Priestly, 1993]. Moreover, the first order schemes show characteristics which are to be found in equivalent higher order schemes. Arguments for thorough investigation of first order methods are numerous.

3.2.2 Conservation

When the wind speed U is constant and when we use periodic boundary conditions, we have the conservation property

$$\frac{\partial}{\partial t}\int_0^L \psi^k \, dx = 0\,, \tag{3.13}$$

for any integer k. We say that the kth moment of ψ is conserved. In the analytical case any moment of ψ is conserved. It is desirable that discrete analogs of (3.13) are fulfilled as well. The following theorem demonstrates that the first moment is trivially conserved[6].

Theorem 2 *Consider the general three point semi-Lagrangian scheme* (3.8) *and suppose the domain is of length* $M\Delta$. *Furthermore, assume periodic boundary conditions. If* $A_1 + A_2 + A_3 = 1$, *then the scheme has the discrete conservation property*

$$\sum_{I=0}^{M-1} \phi_I^{n+1} = \sum_{I=0}^{M-1} \phi_I^n\,.$$

In general conservation of higher moments of ψ is not guaranteed.

[6] the proof is given in appendix A.4

Second moment conservation

Define the schemes deviation from conservation of the second moment of ψ, denote the error $\mathcal{E}$, as

$$\mathcal{E} \equiv \sum_{i=0}^{M-1} \{\phi_i^n\}^2 - \sum_{i=0}^{M-1} \{\phi_i^{n+1}\}^2 . \tag{3.14}$$

Substitute the formula for consistent three point schemes (3.8) into (3.14) and rearrange terms using periodic boundary conditions. Then the error, $\mathcal{E}$, can be rewritten as

$$\boxed{\mathcal{E} = 2\mathcal{P}\left(2A_1 - \hat{\alpha} - \hat{\alpha}^2\right) + 4\,\mathcal{Q}\,A_1\left(\hat{\alpha} - A_1\right)} , \tag{3.15}$$

where

$$\begin{aligned} \mathcal{P} &\equiv \sum \left[\phi_i^n \cdot \left(\phi_i^n - \phi_{i+1}^n\right)\right] , \\ \mathcal{Q} &\equiv \sum \left[\phi_i^n \cdot \left(\tfrac{3}{2}\phi_i^n - 2\phi_{i+1}^n + \tfrac{1}{2}\phi_{i+2}^n\right)\right] , \end{aligned}$$

where the sum is from $i = 0$ to $M - 1$.

Solving the quadratic equation

$$\mathcal{E} = 0 , \tag{3.16}$$

for A_1 (at each time level) will yield a scheme which conserves $\sum \phi^2$. The two solutions of (3.16) are

$$A_1 = \frac{\mathcal{P} + \hat{\alpha}\,\mathcal{Q} \pm \sqrt{\mathcal{P}^2 + \hat{\alpha}^2\mathcal{Q}^2 - 2\,\hat{\alpha}^2\,\mathcal{P}\mathcal{Q}}}{2\mathcal{Q}} . \tag{3.17}$$

Either value of A_1 can not be eliminated using stability arguments, since by conservation the solution is bounded. Instead, consider the special case where the departure

point coincides with grid points, i.e. $\hat{\alpha} = 0$. Equation (3.17) reduces to

$$\frac{\mathcal{P} \pm \mathcal{P}}{2\,\mathcal{Q}}. \tag{3.18}$$

If A_1 vanishes, the numerical solution will be exact. This suggests that choosing the minus solution in (3.17) is the physically relevant one. Test simulations advecting various profiles (isolated waves as well as more complicated initial conditions) for arbitrary $\hat{\alpha}$ values support this choice. Hence, the plus solution in (3.17) is definitely eliminated.

Although the conservative scheme will turn out to be rather theoretical, because of intrinsic problems with extending the method to higher dimensions and non-trivial flows, some interesting observations may be made. For the moment restrict the analysis to a very simple situation.

Pure waves

Consider the isolated wave of domain length, $M\Delta$. It is obvious that $\mathcal{E}$ and the squared modulus of the amplification factors deviation from neutral damping, $1 - \|\Gamma\|^2$, are proportional. Nevertheless, a mathematical proof of the latter statement will be given, since extrapolation of the results may be used to interpretate the second moment conservative scheme when applied to arbitrary distributions.

First of all, note the similarity in form between (3.15) and the deviation from neutral damping,

$$1 - \|\Gamma\|^2 = 2c\left(2A_1 - \hat{\alpha} - \hat{\alpha}^2\right) + 4A_1c^2\left(\hat{\alpha} - A_1\right).$$

This observation motivates the following lemma.

Lemma 3 *For the $M\Delta$ wave defined on a periodic domain of length $M\Delta$ we have*

$$\frac{c}{\mathcal{P}} = \frac{2}{M} \quad \textit{and} \quad \frac{c^2}{\mathcal{Q}} = \frac{2}{M}.$$

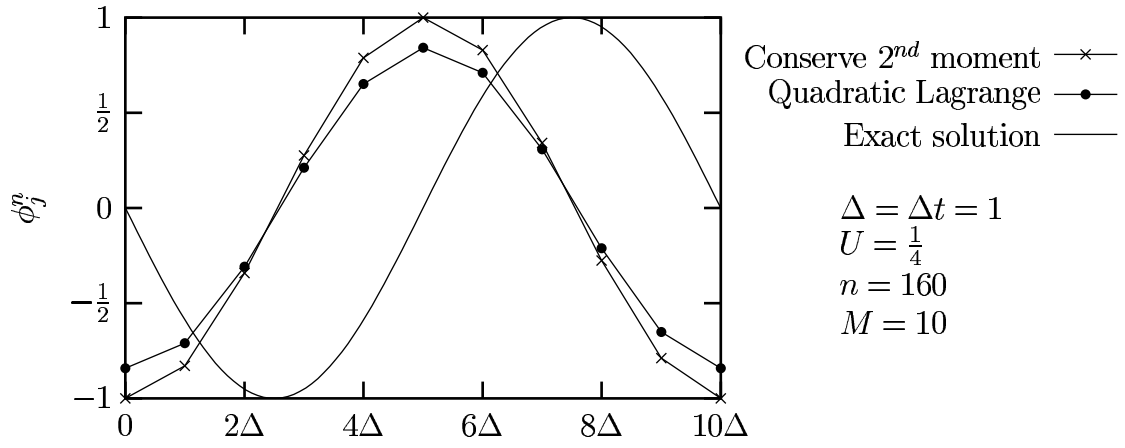

Figure 3.3: The 10Δ wave after four complete translations of the periodic domain using a three point semi-Lagrangian scheme with interpolation conserving ψ^2 and the conventional semi-Lagrangian scheme. All dimensional variables are written in SI units.

Insertion into the formulas of $\mathcal{E}$ and $1-||\Gamma||^2$ proves the proportionality. From lemma 3 we have

$$\frac{2\pi\,\Delta}{L} = \cos^{-1}\left(1-\frac{\mathcal{Q}}{\mathcal{P}}\right), \tag{3.19}$$

i.e. given the grid point values of an arbitrary pure wave one can, with the aid of $\mathcal{P}$ and $\mathcal{Q}$, compute the wavelength of the pure wave. Note that there exists no choice of A_1 for which the scheme conserves ψ^2 for arbitrary wavelengths. To find an A_1 value for which the scheme is neutrally damping one must solve (3.17). As can be depicted from figure 3.1, we must leave the unconditionally stable interval defined in lemma 1 to find a neutrally damping[7] value of A_1. Figure 3.3 shows the 10Δ wave advected 160 time steps using a three point semi-Lagrangian scheme conserving ψ^2 and, for comparison, the conventional quadratic semi-Lagrangian solution. In principle, the algorithm recognizes the isolated wave (finds c) and can thereby choose a neutrally damping value of A_1, for example by equation (3.9), as if we knew the wavelength beforehand. Evidently, the scheme is neutrally damping but more dispersive than the

[7]unless the pure wave is the 2Δ wave and $A_1 = A^+$ or $\hat{\alpha} = 0$ (see figure 3.1)

Interpolation method	(a) E_{DISS}	E_{DISP}	(b) E_{DISS}	E_{DISP}
Conservation of 2^{nd} moment	0.12(-16)	0.97	0.30(-18)	0.33(-1)
Quadratic Lagrange	0.12(-1)	0.79	0.18(-3)	0.28(-1)
Least squares	-	-	0.41(-1)	0.12(-1)

Table 3.1: (a) E_{DISS} and E_{DISP} after 160 time steps advecting the 10Δ wave (see figure 3.3) and (b) after 200 time steps advecting the sine squared wave (see figure 3.4).

conventional semi-Lagrangian scheme.

Arbitrary distributions

A simulation of a less trivial test profile has been performed. To judge the results by other means than their degree of being visually pleasing, some calculable measure of error is used. The variable chosen to make the analysis quantitative is the mean-square error. Following [Takacs, 1985], the mean-square error is divided into two parts, one indicative of dissipation error, E_{DISS}, and one indicative of the dispersion error, E_{DISP},

$$\frac{1}{M}\sum_{j=0}^{M-1}\left(\phi_j^n - \psi_j^n\right)^2 = E_{DISS} + E_{DISP}\,,$$

where

$$E_{DISS} = \left[\sigma\left(\phi\right) - \sigma\left(\psi\right)\right]^2 + \left(\overline{\phi} - \overline{\psi}\right)^2\,, \tag{3.20}$$

$$E_{DISP} = 2\left(1-\rho\right)\sigma\left(\phi\right)\sigma\left(\psi\right)\,, \tag{3.21}$$

where ψ_j^n is the analytical solution evaluated at time $n\Delta t$ and at x value $j\Delta$. $\overline{(\,)}$ denotes the mean value, $\sigma(\,)$ the standard deviation and ρ the correlation coefficient between the numerical and analytical solution on the set of grid points: 0, Δ, ...,$(M-1)\,\Delta$.

Note that when two wave patterns differ only in amplitude, but not in phase, their correlation coefficient ρ is one. According to (3.21), $E_{DISP} = 0$, which is a reasonable result.

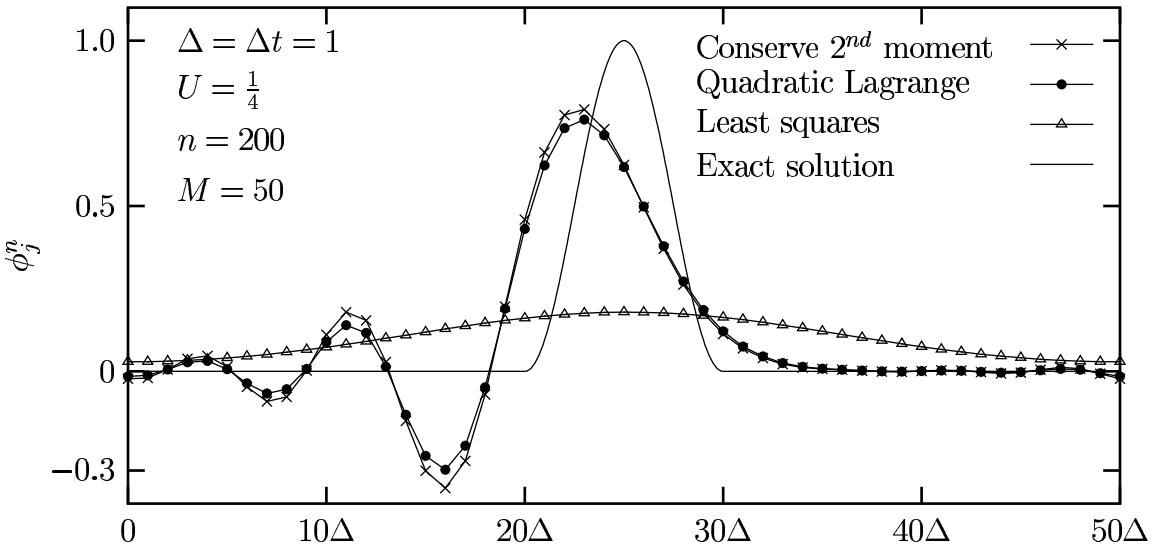

Figure 3.4: Integrating the one-dimensional advection equation for 200 time steps using different three point methods. The initial condition is a sine squared wave. The legends indicate interpolation method used. All dimensional variables are given in SI units.

In table 3.2.2(a) E_{DISS} and E_{DISP} are listed for the simulation of the 10Δ wave. As expected, the dissipation error E_{DISS} indicates neutral damping and E_{DISP} confirms increased dispersion for the conservative scheme.

The second simulation is the advection of a less simple test profile

$$\psi(x) = \begin{cases} 0 & \text{for } 0 \leq x < 20\Delta \\ \sin^2\left(\frac{\pi(x-20\Delta)}{10\Delta}\right) & \text{for } 20\Delta \leq x \leq 30\Delta \\ 0 & \text{for } 30\Delta < x < 50\Delta\,, \end{cases}$$

which consists of a sine-squared wave of width 10Δ. ψ as well as all its derivatives are continuous guaranteeing a smooth initial distribution. The profile has strong gradients, which is often of great challenge for the numerical scheme. Figure 3.4 shows the sine-squared wave after one complete translation of the periodic domain using different interpolators. The corresponding errors associated with dissipation and dispersion are to be found in table 3.2.2(b). Note that the dissipation error of

the ψ^2 conservative scheme is negligible. The same result as for pure waves. As expected, the least squares interpolator is excessively damping, reducing the initial profile to a near constant.

The value of A_1 may vary during the integration process using the conservative scheme. Slight monotonic increase from the value of 0.15371 to 0.154232 is observed. These values are slightly outside the unconditional stable interval $[A^- = 0.15625, A^+ = 0.62500]$ of A_1 values.

The $\mathcal{P}$ and $\mathcal{Q}$ values, which are part of the conservative algorithm, might be used together with the results of section 3.2.2 to give a generalized interpretation of the A_1 value yielding conservation of the second moment of ψ. Although the results of lemma 3 are derived for pure waves only, one could extrapolate by substituting $\mathcal{P}$ and $\mathcal{Q}$ into equation (3.19) to find the pure wavelength for which the scheme is neutrally damping. The wavelength found using the above extrapolation increases monotonically from a value of $10.56\,\Delta$ to $11.88\,\Delta$ during the simulation. So the neutrally damped wavelength chosen by the algorithm seems to describe the scale of the disturbance. Figure 3.5 shows the squared modulus of the amplification factor as a function of wavelength for the start and end value of A_1 calculated during the simulation (for comparison also for the value of A_1 yielding the 2nd-order conventional semi-Lagrangian scheme). The conservative scheme is slightly unstable for longer wavelengths and less dissipative than the conventional semi-Lagrangian scheme for shorter wavelengths.

Once an A_1 value is chosen, the scheme will be neutrally damping for the particular wavelength, as described in the above interpretation of the conservative choice of A_1. The distribution is, however, a superposition of many wavelengths. Hence, dispersion will be present as the class of semi-Lagrangian schemes are unable to produce equal or no phase errors at all wavelengths for a fixed A_1 value (see figure 3.2). From figure 3.4 it is apparent that the dispersion errors of both the conventional semi-Lagrangian scheme as well as the ψ^2 conservative one produce strong trailing waves. Qualitatively, these trailing waves are identical though slightly more damped using the conventional Lagrange interpolant. As the waves disperse, undershoots and overshoots are produced. Furthermore, the shape of the initial profile is distorted.

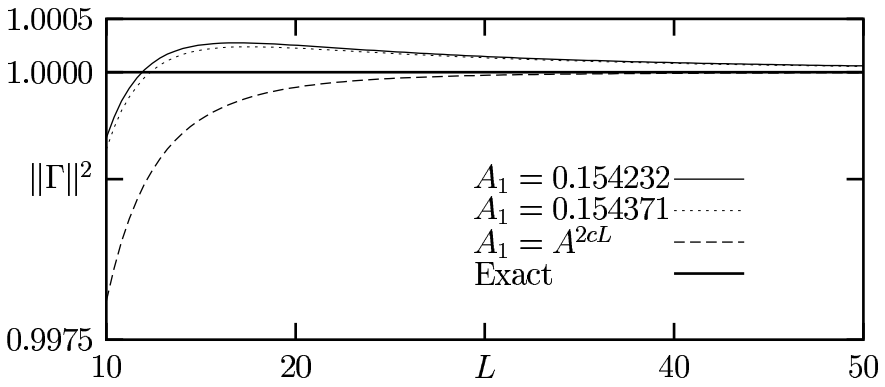

Figure 3.5: The squared modulus of the amplification factor as a function of wavelength, L, given in units of Δ for selected A_1 values.

This indicates that closely related to dispersion errors is the concept of monotonicity. Modeling physical quantities monotonicity (or rather the lack of it) gives rise to great concern and deserves a section of its own.

3.2.3 Monotonicity

If ψ represents the concentration of chemical constituents, humidity or any other positive definite quantity, the results obtained with the conventional semi-Lagrangian scheme and the conservative scheme pose major conceptional problems. The numerical advection scheme erroneously produces areas where the field is negative, contradicting underlying physics. Negative humidity or concentrations are, of course, not physical acceptable. Less noticeable, but equally serious, are areas of overshooting. For example, if the concentration of water vapor during an overshoot erroneously supersaturates, irreversible physical parameterizations are invoked. This might result in spurious precipitation if the advection scheme is part of a forecast model.

It is quite clear that undershoots and overshoots might trigger physical processes to spurious behavior which alter the subsequent evolution of the system. Special care to try to avoid this unfortunate behavior is highly recommended, if not a necessity.

Spurious numerical oscillations in regions of steep gradients of the interpolated variables are eliminated if the scheme is monotone. A monotone scheme is free of

undershoots and overshoots, since monotonicity by definition prevents the formation of new extrema. The class of linear monotone schemes is, however, very limited. Godunov's theorem [Godunov, 1959], which states that any linear, monotone scheme is of most first order accurate, excludes the majority of feasible schemes. Note that even if the scheme is only of first order, monotonicity is not guaranteed. Requiring preservation of monotonicity sacrifices accuracy to such an extent that in many applications these schemes are condemned useless. Nevertheless, selective use of linear schemes in numerical algorithms can make the highly diffusive first order methods feasible for practical use as discussed in section 3.2.1.

The consistency requirements (3.7) guarantee first order accuracy and keeping A_1 not equal to A^- implies less than 2nd-order accuracy. Hence, there is no conflict with Godunov's theorem but, as already noted, a linear scheme is not necessarily monotone. This will be demonstrated in the coming monotonicity analysis of the general three point semi-Lagrangian scheme.

By definition, a finite difference scheme expressed in functional form

$$\phi_I^{n+1} = \mathcal{H}\left(\phi_{I-N^-}, ..., \phi_{I+N^+}\right) ,$$

is monotone if

$$\frac{\partial \mathcal{H}\ \left(\phi_{I-N^-}, ..., \phi_{I+N^+}\right)}{\partial \phi_i} \geq 0 ,$$

for each integer i in the interval $[I - N^-, I + N^+]$. For the general three point semi-Lagrangian scheme (3.3) the condition for monotonicity is simply

$$A_j \geq 0 \quad \text{for} \quad j = 1, 2, 3 .$$

Using the consistency equations (3.7) and that A_1 has to be non-negative, the finite difference formula is monotone if and only if the value of A_1 is restricted to

$$\max\left(0, \hat{\alpha}\right) \leq A_1 \leq A^+ .$$

Note that if $\hat{\alpha} \geq 0$ then $A^{1cL} = \hat{\alpha}$. Looking at amplification properties on figure 3.1 it

is evident that any value of A_1 larger than A^{1cL} will worsen the overall amplification properties. So, in terms of dissipation properties, the conventional linear Lagrangian scheme is the optimal monotonicity-preserving scheme. Again, phase properties may be improved while keeping the scheme monotone, but with the consequence of major increase in overall damping.

Fixers

In order to suppress monotonicity violating overshoots and undershoots characteristic of quadratic and higher order interpolation schemes, one may adopt linear interpolation in regions of step gradients [Bermejo and Staniforth, 1992]. The *quasi-monotone* algorithm presented in [Bermejo and Staniforth, 1992] alters the high order interpolation if it overshoots or undershoots. The method has very straightforward implementation: After the high order non-monotone interpolation, the resulting value is restricted to stay within the interval bounded by the two surrounding grid point values of ψ used during the fit.

In this context, the altering of grid point values may be viewed as a modification of the A_1 value. A consequence of altering A_1 values is that conservation of first moment might be violated. Again, a good example of how improvement of one property is invoked at the expense of another. Furthermore, fixers may introduce excessive numerical diffusion that smears out sharp features of the interpolated fields. It is, however, a necessity to use fixers if a scheme produces non-physical values during undershoots, unless the scheme is intrinsically positive definite.

3.3 Higher order schemes

By using more than three points during the interpolation process, the formal accuracy may be increased to more than first order. In a N point scheme the requirement of at least $(N-2)$th-order accuracy results in one free parameter. Hence, an analysis that in principle is identical to the one of the three point scheme can be carried out. We will consider up to at least 4th-order accurate schemes i.e. up to $N = 6$.

3.3.1 The schemes

Consider an N point scheme on the form (3.3). The definitions of $N^{\pm}$, p and $\hat{\alpha}$ are unchanged. Following the procedure for obtaining at least $(N-2)$th-order accuracy, outlined in section 3.1.1, one obtains a family of schemes which all have similar forms. They can all be split into a part which is identical to a $(N-2)$th-order Lagrange interpolation[8], denote it $\mathcal{L}$, and a product between the free parameter A_1 and a rest term, which will be denoted $\mathcal{R}$. That is

$$\phi_I^{n+1} = \mathcal{L} + \mathcal{R} \cdot A_1 \,,$$

where $\mathcal{L}$ uses $\phi^n_{I-p-N^-+1}$, $\phi^n_{I-p-N^-+2}$, ..., $\phi^n_{I-p+N^+}$ for the interpolation[9]. The rest term, $\mathcal{R}$, is given by

$$\mathcal{R} = \begin{cases} \phi^n_{I-2} - 3\,\phi^n_{I-1} + 3\,\phi^n_I - \phi^n_{I+1} & \text{for} \quad N=4 \\ \phi^n_{I-2} - 4\,\phi^n_{I-1} + 6\,\phi^n_I - 4\,\phi^n_{I+1} + \phi^n_{I+2} & \text{for} \quad N=5 \\ \phi^n_{I-3} - 5\,\phi^n_{I-2} + 10\,\phi^n_{I-1} - 10\,\phi^n_I + 5\,\phi^n_{I+1} - \phi^n_{I+2} & \text{for} \quad N=6. \end{cases}$$

3.3.2 Stability analysis

The amplification factor and the relative phase speed are obtained by a standard Von Neumann analysis (see section 2.2). Again, the formulas can be split into a part related to the Lagrange interpolation and a part related to the rest term $\mathcal{R} \cdot A_1$

$$||\Gamma||^2 = ||\Gamma_{\mathcal{L}}||^2 + ||\Gamma_{\mathcal{R}}||^2 \,,$$

where $||\Gamma_{\mathcal{L}}||^2$ is the squared modulus of the amplification factor resulting from the Lagrange interpolation $\mathcal{L}$. $||\Gamma_{\mathcal{R}}||^2$ is a rest term[10] introduced by $\mathcal{R} \cdot A_1$. Explicit

[8] but, in general, *not* identical to the Lagrange interpolant of a conventional scheme (the central point x_{I-p} for the two interpolations are not always identical)

[9] the explicit formulas for $\mathcal{L}$ can be found in appendix A.5

[10] Γ_R is *not* the amplification factor of the scheme $\phi_I^{n+1} = \mathcal{R} \cdot A_1$

formulas for $||\Gamma_{\mathcal{L}}||^2$ and $||\Gamma_{\mathcal{R}}||^2$ for up to six point schemes can be found in appendix A.5 as well as the explicit formulas for the relative phase speeds.

In order to be able to visualize stability properties, consider two situations: One where the departure point is located $\frac{1}{4}\Delta$ upstream from x_I, and another where x_* is located $\frac{3}{4}\Delta$ upstream from x_I. Plotting isolines of $||\Gamma||^2$ and R as a function of (A_1, δ) for the selected departure points using the four point scheme (figure 3.6), five point scheme (figure 3.7) and six point scheme (figure 3.8), one quickly notices that all schemes show similar stability properties in a qualitative sense. Therefore the variables A^+, A^-, A^*, $A^{j\,\mathcal{LS}}$ ($j = N-2$) and $A^{j\,cL}$ ($j = N-1$ or $j = N-2$), introduced during the three point analysis to mark A_1 values resulting in schemes of interest or qualitative changes in stability, can be used equivalently for this analysis. That is, $A^{\pm}$ refer to the maximum and minimum unconditionally stable value of A_1. As in the three point case we find that all schemes damp the 2Δ wave completely at $A_1 = A^*$. A_1 values resulting in schemes of interest are denoted with superscripts $\mathcal{LS}$ or cL referring to least squares schemes or conventional semi-Lagrangian schemes. The numbers in the superscript refer to the formal order of accuracy of the schemes. For example, $A^{3\,\mathcal{LS}}$ refers to the A_1 value resulting in the 3rd-order least squares scheme. Explicit formulas for all of the before mentioned values of A_1 are listed in appendix A.5 for the four, five and six point schemes.

Symmetry in the amplification factor As may be noticed on figures 3.6, 3.7 and 3.8, the squared modulus of the amplification factor, $||\Gamma||^2$, which is a function of the free parameter A_1, the interpolary parameter $\hat{\alpha}$, and the wavelength expressed in terms of c (we will write $||\Gamma(A_1, \hat{\alpha}, c)||^2$), has the following symmetry property

$$\left\|\Gamma\left(A^-\big|_{\hat{\alpha}} + \Delta A, \hat{\alpha}, c\right)\right\|^2 = \begin{cases} \left\|\Gamma\left(A^+\big|_{1-\hat{\alpha}} - \Delta A, 1-\hat{\alpha}, c\right)\right\|^2 & \text{for } N \text{ even} \\ \left\|\Gamma\left(A^-\big|_{-\hat{\alpha}} + \Delta A, -\hat{\alpha}, c\right)\right\|^2 & \text{for } N \text{ odd,} \end{cases}$$

where ΔA can be any real number and $A^{\pm}\big|_x$ signifies the evaluation of $A^{\pm}$ replacing $\hat{\alpha}$ with x in the formula for $A^{\pm}$.

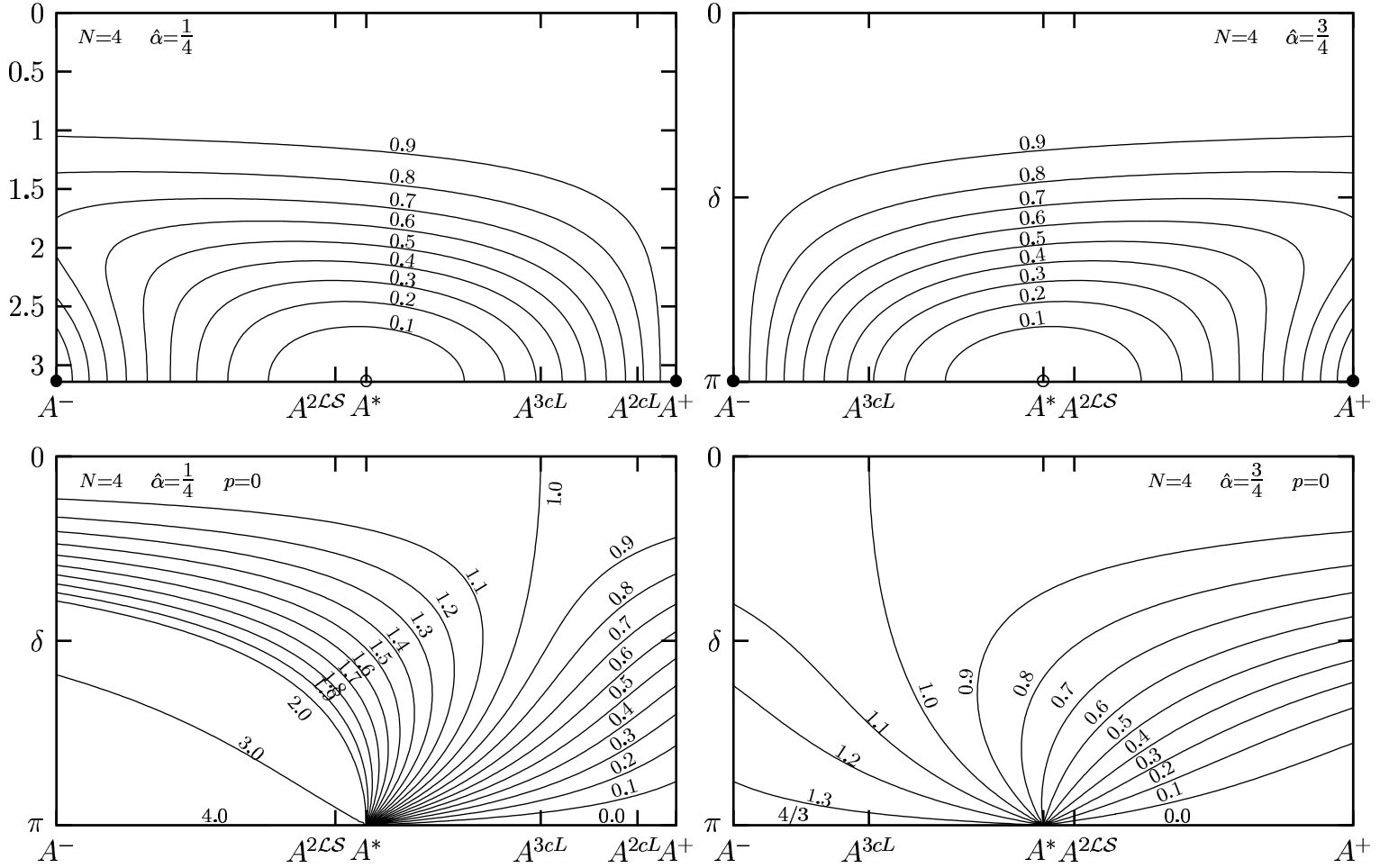

Figure 3.6: (Four point schemes) Plots on the first/(second) row show: Isolines of the squared modulus of the amplification factor/(relative phase speed) as a function of A_1 and δ for fixed $\hat{\alpha}$ and p values (their values are printed on each plot). The circles/(bullets), $\circ$/($\bullet$), mark the points where the scheme is completely/(neutraly) damping.

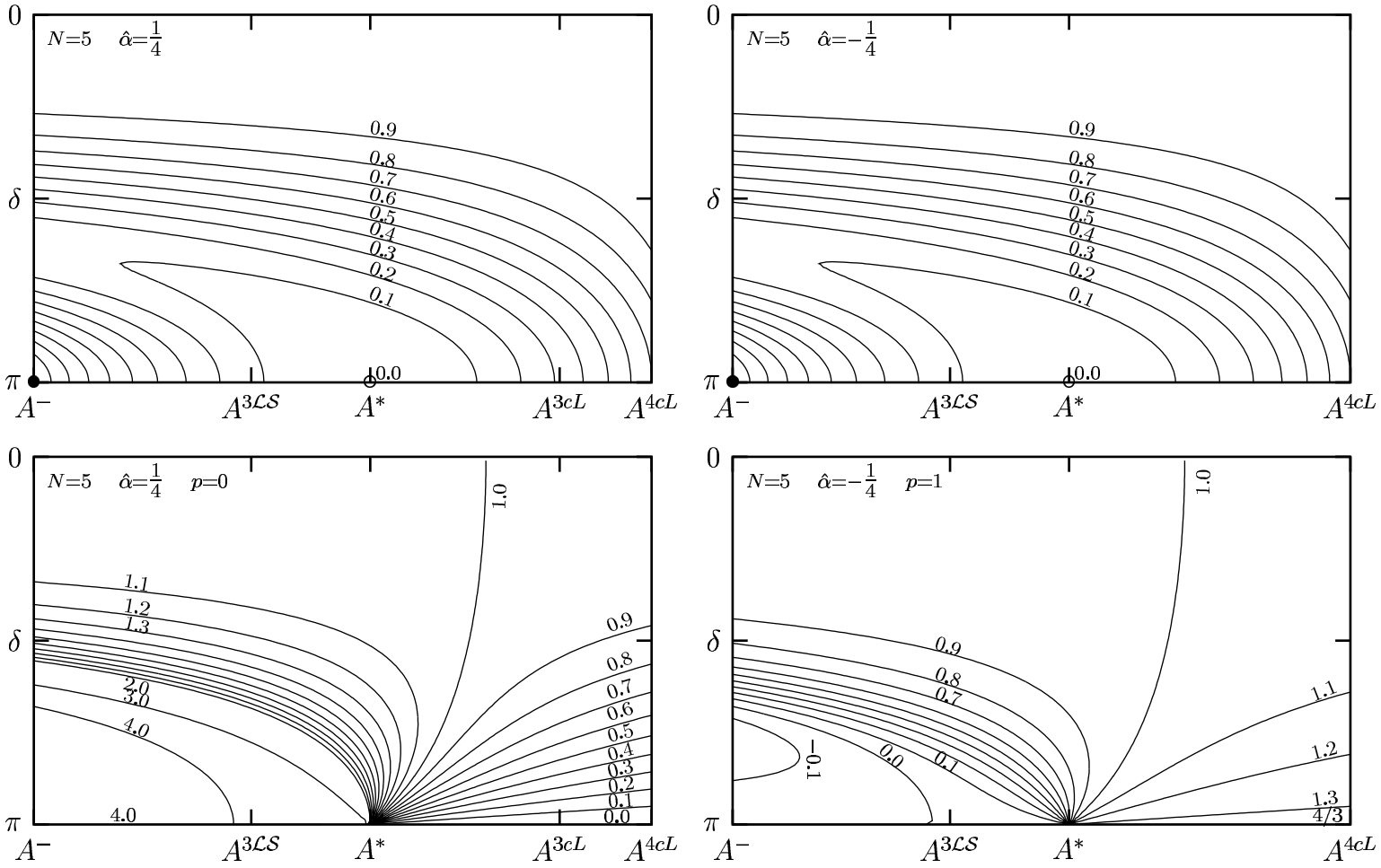

Figure 3.7: (five point schemes) Plots on the first/(second) row show: Isolines of the squared modulus of the amplification factor/(relative phase speed) as a function of A_1 and δ for fixed $\hat{\alpha}$ and p values (the values are printed at the top of each plot). The circles/(bulets), $\circ$/($\bullet$), mark the points where the scheme is completely/(neutraly) damping. Note $A^+ = A^{4cL}$.

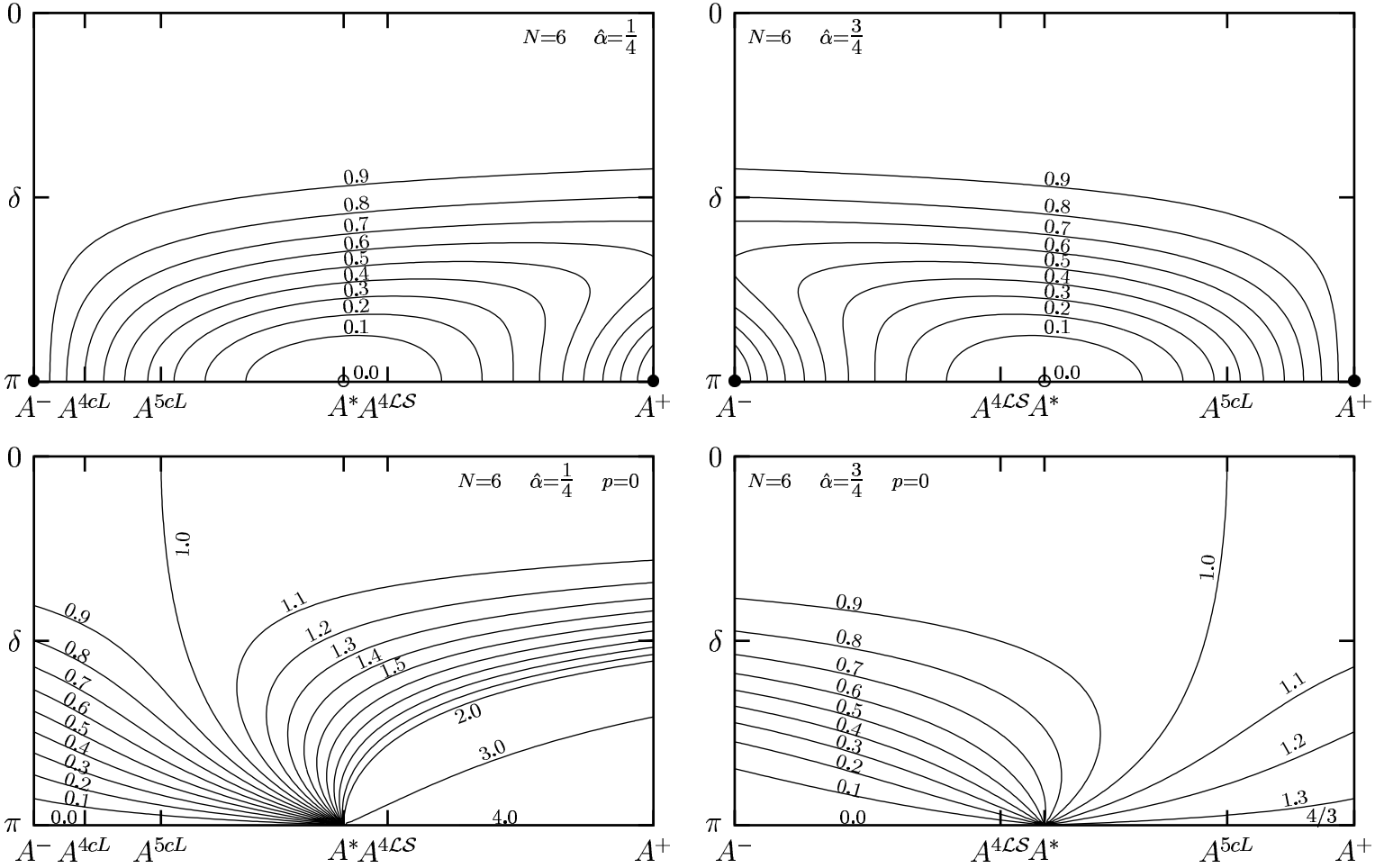

Figure 3.8: (Six point schemes) Plots on the first/(second) row show: Isolines of the squared modulus of the amplification factor/(relative phase speed) as a function of A_1 and δ for fixed $\hat{\alpha}$ and p values (the values are printed at the top of each plot). The circles/(bulets), $\circ$/($\bullet$), mark the points where the scheme is completely/(neutraly) damping.

Optimal amplification properties During the analysis of the three point scheme it was noticed that the A_1 yielding maximum accuracy corresponded to the $(N-1)$th-order conventional semi-Lagrangian scheme. Furthermore, this A_1 value was located at one of the end points of the interval of A_1 values, securing unconditional stability. When using more points for the interpolation, these observations are only correct if N is odd.

Let N be even. In that case $A^{(N-1)\,cL}$ is located in the interior of $[A^-, A^+]$ and does not yield superior amplification properties. Note also that the $(N-2)$th-order conventional semi-Lagrangian scheme has dissipation properties superior to the $(N-1)$th-order conventional scheme. The A_1 value generating a scheme with overall superior dissipation properties is to be found at either A^+ or A^-, depending on the sign of $\hat{\alpha}$. More precisely, an optimal choice of A_1 value regarding overall amplification properties is to be found at

$$A_1 = \begin{cases} A^- & \text{for } \hat{\alpha} < \frac{1}{2} \quad (N \text{ even}) \\ A^+ & \text{for } \hat{\alpha} > \frac{1}{2} \quad (N \text{ even}), \end{cases}$$

For a given N, choosing A_1 equal to $A^{(N-1)\,cL}$ defines a scheme with near optimal phase speed properties for longer wavelengths. Note that the isoline indicating exact relative phase speed, $R = 1$, converges towards $A^{(N-1)\,cL}$ in the long wave limit.

The relative phase speed of the 2Δ wave As in the three point case, for fixed $\hat{\alpha}$ and p values the relative phase speed of the shortest resolvable wave can take two constant values, either R^+ or R^-, depending on the value of A_1. These limit values of R do not depend on N. Again, the range of A_1 values for which the relative phase speed is equal to R^+, and the range of A_1 values for which R is equal to R^-, are separated by $A_1 = A^*$. However, if for example A_1 is less than A^*, it is dependent on N whether R will take the value R^+ or R^-. See appendix A.5 for details concerning the four, five and six point schemes. About the performance of the scheme with respect to phase errors in the 2Δ wave limit, one may generally conclude: If N is

even, then

$$R^- \text{ is always closer to one than } R^+ \text{ for } \hat{\alpha} < \tfrac{1}{2}\,,$$
$$R^+ \text{ is always closer to one than } R^+ \text{ for } \hat{\alpha} > \tfrac{1}{2}\,.$$

For odd N, R^- is always closer to one than R^+. On figures 3.6, 3.7 and 3.8, note that A_1 values resulting in conventional semi-Lagrangian schemes are always located in the interval of optimal limit value of R. Furthermore, note that this is not the case for the least squares schemes.

General comments on stability properties As superior amplification and phase speed properties are not found for equal A_1 value, some kind of compromise must be made if an optimal value must be chosen. It seems plausible that it is located in between the A_1 value yielding optimal dissipation properties and the A_1 value towards which the $R = 1$-isoline converges in the long wave limit. Note that the least squares schemes are always outside this interval and that A_1 values yielding conventional semi-Lagrangian schemes are always located in this interval.

3.3.3 Beyond the stability analysis

In order to try to gain a more practical understanding on how the more general schemes perform in situations more complicated than the pure wave case, a series of advection experiments have been performed. In conventional semi-Lagrangian schemes the 3rd-order interpolator is often selected, since it seems to be a good compromise between accuracy and computational efficiency [Staniforth and Côté, 1991]. Therefore we choose the general five point scheme, which is at least 3rd-order accurate, for the advection experiments. In literature, numerous simple profiles have been used for numerical tests of the performance of schemes of interest: For example, the rectangular wave, Gaussian distribution, sine squared cone and the irregular signal described in [Smolarkiewicz and Gabowski, 1990]. In the coming advection tests, qualitatively similar results are obtained when advecting all these distributions. Using the rectangular wave as initial condition, the errors are more apparent and serves well for illustrative purposes. Therefore we will focus on this distribution

although geophysical fields of interest might have quite different distributions. One should, however, keep in mind that a scheme may perform miserably using one test function and work very well with other test distributions (an example is given in [Ostiguy and Laprise, 1990]). Therefore results of simple advection tests should be taken with a grain of salt.

A $10\,\Delta$ wide rectangular wave is advected 200 time steps on a domain of length 50Δ with constant wind speed corresponding to $\hat{\alpha} = \frac{1}{4}$ and $p = 0$. The initial distribution, after having been advected one domain length using the five point scheme, is depicted on figure 3.9(a,b,c) for selected A_1 values. Also to be found on one of the plots on figure 3.9 is the mean square error, E_{DISS} and E_{DISP} as a function of A_1.

The numerical solution, after one complete translation of the domain, undergoes a series of qualitative changes in shape as a function of A_1. In a narrow interval starting at A^-, the solution is exceedingly noisy (figure 3.9(a)). Increasing the A_1 value a bit makes the solution smooth and free of small scale noise. Increasing A_1 even further improves the schemes ability to localize the discontinuity of the true solution (figure 3.9(b)). Note also that the solution is symmetric around $x = 25\Delta$. This symmetry is broken by further increase in the A_1 value ($A_1 > A^{3cL}$) and stronger trailing waves develop (figure 3.9(c)). On the plot of the practical measures of total error, dissipation error and dispersion error (mse, E_{DISP} and E_{DISS}), it may be noticed that an increase in A_1 improves all of the three before mentioned error measures, except in a narrow interval starting somewhere in between A^{3cL} and A^+. The minimum in E_{DISP}, $A_1 = A^{opt}$, is located at an A_1 value larger than the optimal value of A_1 for the phase speed representation observed during the Von Neumann analysis. E_{DISS} decreases monotonically as a function of A_1, as was also observed for the amplification factor for wavelengths longer than the 3Δ wave. Note that the error representative of numerical dissipation is approximately one order of magnitude less than the dispersion error, E_{DISP}. Increasing A_1 to the largest unconditionally stable value improves E_{DISS} even more but the trailing waves start to disrupt the shape of the solution. On figure 3.10 measures of the conservation of first and second moment of ψ are plotted, as well as the maximum overshoot and undershoot. The scheme automatically conserves mass as has been proven for the three point scheme. Second

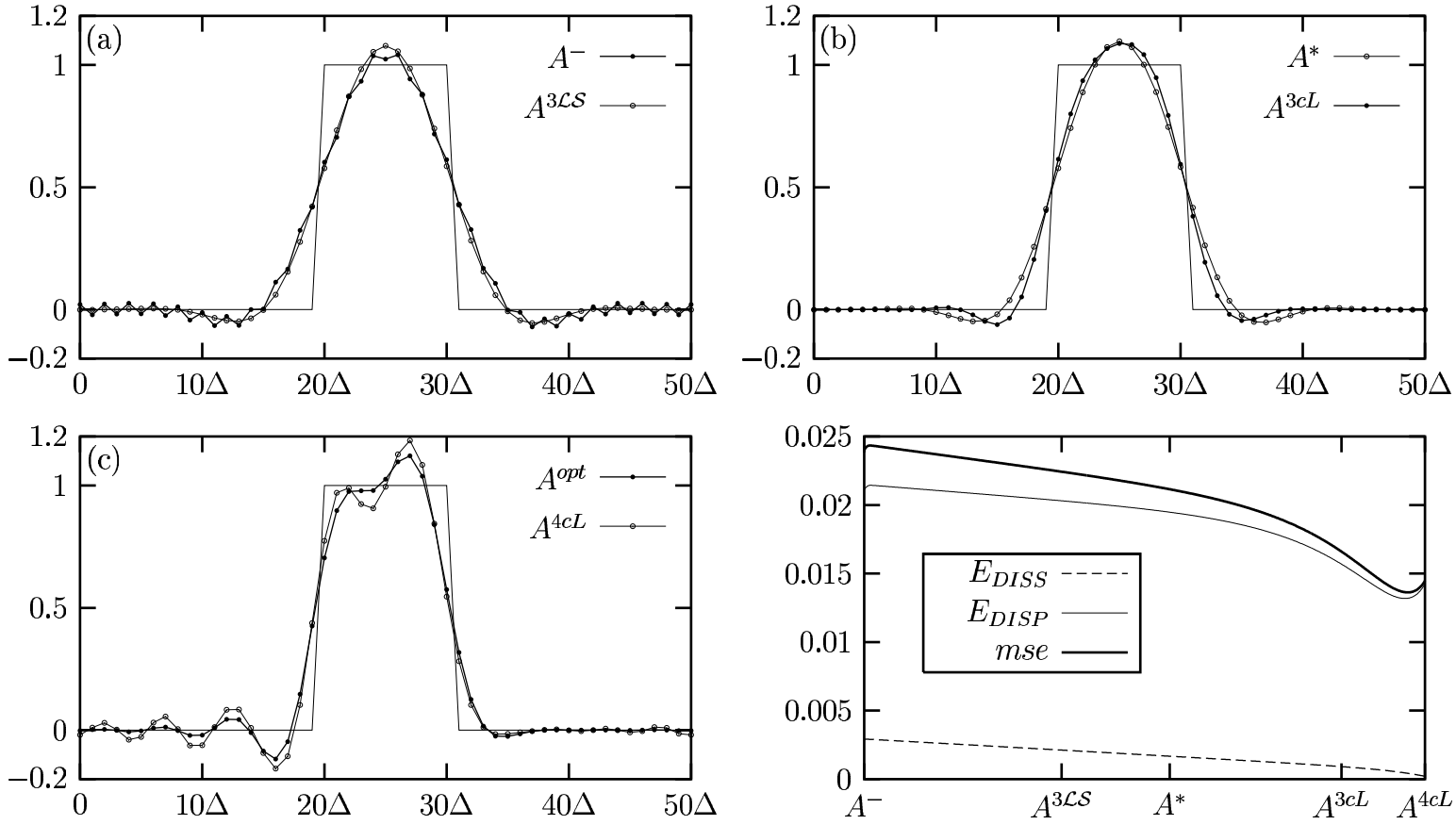

Figure 3.9: (a,b,c) Results of advection tests for selected A_1 values using the five point scheme and a rectangular wave as initial distribution ($n = 200$, $U = \frac{1}{4}$, $M = 50$, N=5). The solid line shows the exact solution. (figure in lower right corner) Mean square error (mse), E_{DISS} and E_{DISP} as a function of A_1 for the advection experiment just described. A^{opt} denotes the A_1 value for which E_{DISP} is minimal.

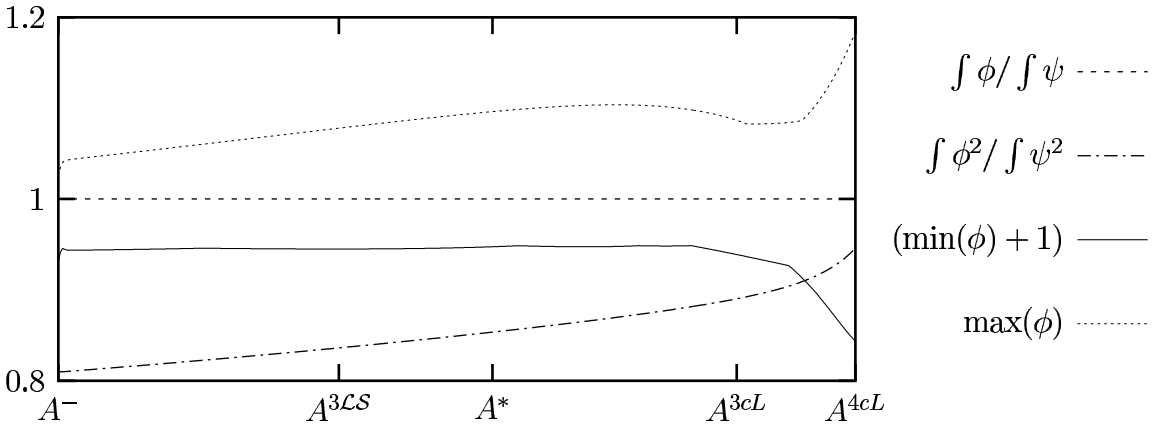

Figure 3.10: The largest overshoot, the largest undershoot, the schemes ability to conserve first and second moment of ψ as a function of A_1 for the advection experiment as described in the caption of figure 3.9.

moment conservation improves for increasing A_1 as was also observed for E_{DISS}. If one increases A_1 so that it exceeds A^+ the scheme will conserve ψ^2. Unfortunately, the trailing waves, which are very strong already for $A_1 = A^+$, will grow even more in amplitude if A_1 is increased beyond A^+. Hence, the 2nd-order conservative scheme is not of any practical interest.

If positive definiteness is indispensable, one may eliminate undershoots by implementing the quasi-monotone algorithm of [Bermejo and Staniforth, 1992] described in section 3.2.3. The numerical advection experiments just described have been performed with this algorithm (see figure 3.11). For $A_1 = A^-$, the noise of the previously observed numerical solution is filtered away. Again, the accuracy improves for increasing A_1, except for a very narrow interval ending at $A_1 = A^+$. Now the minimum in the mean square error and E_{DISP} is smeared out. Furthermore, the error measures (mse, E_{DISS}, E_{DISP}) have increased in magnitude, especially E_{DISS}. The advantages in using the free parameter approach to minimize error measures seem to have been more or less neutralized by the post-adjustment algorithm. With respect to these error measures the 3rd-order and the 4th-order conventional semi-Lagrangian schemes seem to be near optimal.

During the analysis the interpolary parameter has been kept constant. One might

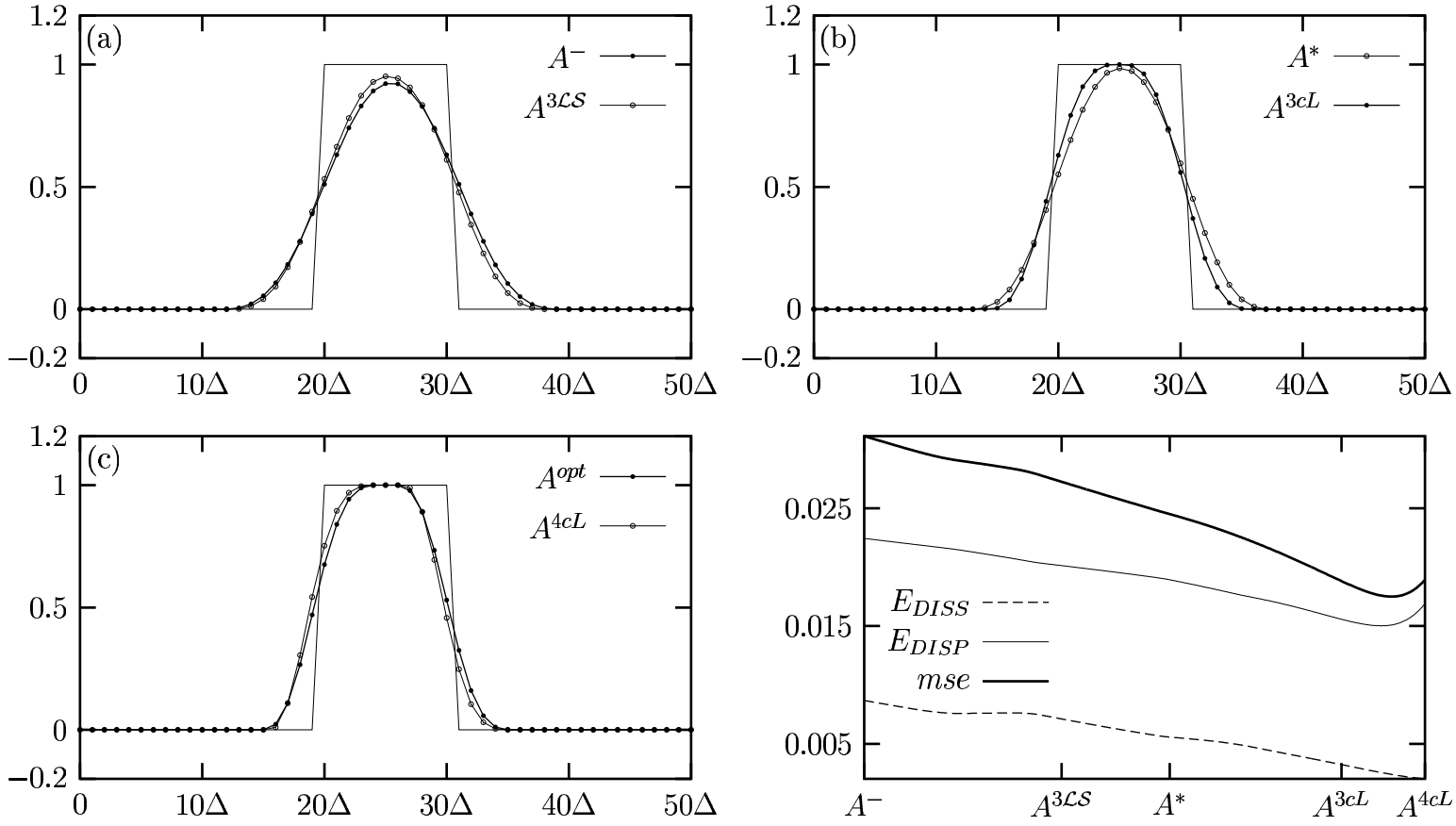

Figure 3.11: Same as figure 3.9, but performing the simulation with the implementation of the quasi-monotone algorithm of [Bermejo and Staniforth, 1992].

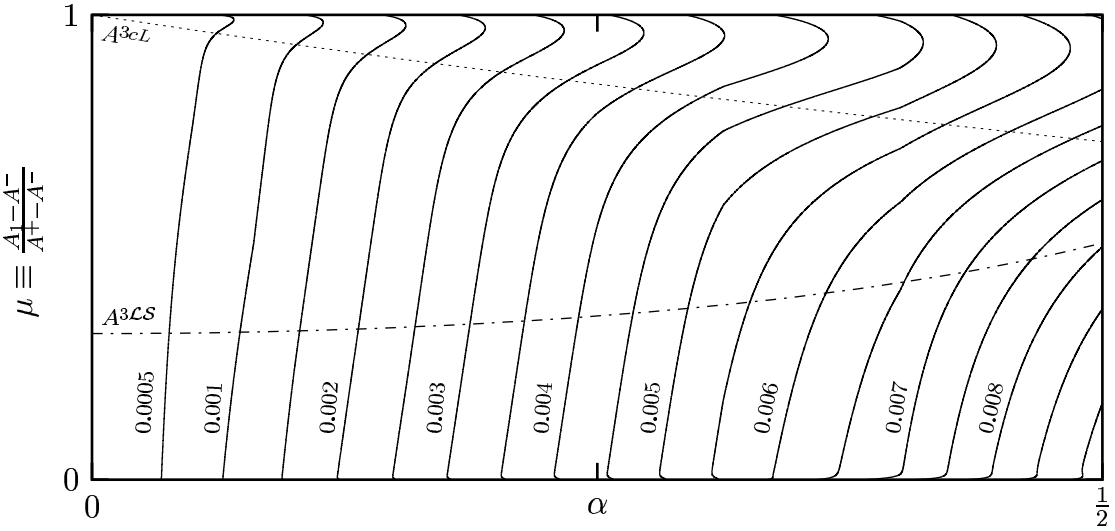

Figure 3.12: Isolines of E_{DISP} as a function of the free parameter α and A_1 (in terms of the dimensionless variable μ) after advecting the 10Δ wide rectangular wave one complete translation of a 50 grid point domain. The dash-dot line mark the A_1 values yielding the 3rd-order least squares scheme, and the dotted line the A_1 values resulting in the 3rd-order conventional semi-Lagrangian scheme. Note that $\mu = 1$ corresponds to $A_1 = A^{4cL}$.

question how the scheme performs at other $\hat{\alpha}$ values. To illuminate this question a simulation similar to the one discussed in [Takacs, 1985] has been performed. Consider the previous setup for the advection experiment without the quasi-monotone algorithm: A 10Δ wide rectangular wave is advected a 50Δ distance, i.e. one complete translation of the domain. The wave is advected for α ranging from 0 to $\frac{1}{2}$ and for A_1 values ranging from the minimum to the maximum unconditionally stable value. Having completed a simulation for given (α, A_1), the dispersion error is calculated and scaled by the maximum mean square error and the number of iterations required to advect the rectangular wave the 50Δ grid point distance. Hence, one gets a more complete picture of how the scheme performs at different wind speeds and A_1 values. The result of the before mentioned simulation is shown on the contour plot on figure 3.12. Note that the tendencies observed during the analysis where $\hat{\alpha}$ was kept fixed are qualitatively identical to the ones observed at other wind speeds. If desired, one could fit the line yielding minimal E_{DISP} to obtain A_1 as a function of

α, providing a scheme which is optimal with respect to E_{DISP}.

Chapter 4

Conclusions

A thorough investigation of the possibilities in improving linear finite-difference semi-Lagrangian schemes to solve the one-dimensional advection equation has been carried out. The starting point of the analysis, the least squares approach, did not provide any significant advantages, but served as a motivator for developing a more general scheme. The class of stable schemes included any linear semi-Lagrangian scheme which use the same number of points for the interpolation, and facilitated comparative analysis between the least squares and conventional approach. Given the number of grid points one wishes to use for the interpolation, it was confirmed that it is possible to construct schemes with slightly improved properties by carefully tuning the free parameter. Nevertheless, the more general analysis strongly suggested that conventional semi-Lagrangian schemes perform quite well, and it might be argued that the additional work required in the free parameter approach is worth while. None of the schemes succeeded in removing spurious ripples and related monotonicity violating phenomena without post adjustment algorithms. A second moment conservative scheme was constructed, but experiments demonstrated that the scheme was not of practical interest.

To be eligible for use in larger models, an advection algorithm must nearly always be at least two-dimensional and possibly also be in spherical geometry. It is not trivial to choose a way of extending a one-dimensional algorithm to two free dimensions[1].

[1] [Williamson and Rasch, 1989] discuss several ways of extending a one-dimensional algorithm to

Suppose that the scheme was extended to two dimensions using a tensor product approach. Then one would have two free parameters, one for each direction of the unit vectors. Conservation of the first moment of ψ for non-divergent flows would no longer be trivial, and it might be possible to take the free parameter approach to advantage. It is, however, beyond the scope of this thesis to analyze extensions to more dimensions.

---

two dimensions

Appendix A

Appendix

A.1 List of symbols

A list of symbols and notation used in this thesis.

$\hat{\alpha}$	Interpolary parameter.
$\hat{a}_i$	Coefficients for the least squares fit used in appendix A.2.
A_1	Free parameter used in the general scheme defined and analysed in chapter 3.
A^+	The maximum value of A_1 for which the general scheme is unconditionally stable.
A^-	The minimum value of A_1 for which the general scheme is unconditionally stable.
A^*	The A_1 value for which the 2Δ wave is completely damped.
$A^{\mathcal{LS}}$	The A_1 value yielding a least square scheme.
A^{cL}	The A_1 value yielding the conventional semi-Lagrangian scheme.
$\mathcal{A}_{\pm}^{(i)}$	Coefficients for the least squares schemes (see table 2.1).
$\mathcal{B}_{\pm}^{(i)}$	Coefficients for the least squares schemes (see table 2.1).
$\mathcal{C}_{\pm}^{(i)}$	Coefficients for the least squares schemes (see table 2.1).
c	Parameter defined to simplify computations: $c \equiv 1 - \cos\delta$.
δ	Parameter defined for convenience: $\delta \equiv k\Delta$.

Δ	Grid spacing.
Δt	Time step.
$\mathcal{D}$	Domain on which the advection equation is solved.
E_{DISP}	Dissipation error (defined in equation (3.21)).
E_{DISS}	Dissipation error (defined in equation (3.20)).
$\mathcal{E}$	Derivation from conservation of ψ^2 (defined in equation (3.14)).
Γ	Amplification factor.
i	Imaginary unit which has the property $i^2 = -1$.
I	Refers to departure point at $I\Delta$.
$\Im$	Function taking the imaginary part of a complex number.
k	Wave number.
L	wavelength.
$\mathcal{L}$	Referring to a Lagrange interpolant.
M	Length of domain is $M\Delta$.
n	Time level.
N^+	Integer used in the definition of the general N point schemes (see equation (3.2)).
N^-	Integer used in the definition of the general N point schemes (see equation (3.2)).
$\mathcal{O}(\,)$	Of order.
p	$I - p$ is the grid point nearest to the departure point.
$\mathcal{P}$	Refers to a sum used in the conservative algorithm (see section 3.2.2).
ϕ	The numerical approximation to the analytical solution ψ.
$\mathcal{Q}$	Refers to a sum used in the conservative algorithm (see section 3.2.2).
R	Relative phase speed.
R^+ or R^-	Relative phase speed of the 2Δ wave.
$\mathcal{R}$	Refers to the rest terms in higher order schemes (see section 3.3.1).
$\Re$	Function taking the real part of a complex number.
sgn( )	Signum function: Equals 1 for positive argument and -1 for negative argument.
U	Wind speed in one dimension.
$\mathbf{v}$	Wind speed vector

x_*	Departure point.
ω	Analytical frequency used in Von Neumann analysis.
ω^*	Numerical frequency used in Von Neumann analysis.
$\overline{()}$	Mean value.

A.2 Method of least squares

Suppose that a q th-order polynomial

$$f(x;\mathbf{a}) = \sum_{\mathrm{r}=0}^{\mathrm{q}} a_{\mathrm{r}} x^{\mathrm{r}} \text{ , where } \mathbf{a} = (a_1, a_2, ..., a_{\mathrm{q}}) \text{ ,}$$

must be fitted through N given points

$$(x_1, y_1), (x_2, y_2), ..., (x_N, y_N) \text{ ,}$$

so that the sum of the squares of the distances of those points from the polynomial is minimum. More precisely, minimize

$$\sum_{\mathrm{i}=1}^{N} [y_{\mathrm{i}} - f(x_{\mathrm{i}};\mathbf{a})]^2 ,$$

with respect to a_{i}. The resulting estimate for $\mathbf{a}$ - denote it $\hat{\mathbf{a}}$ - is obtained by differentiating with respect to a_{i} and setting the result equal to zero

$$\sum_{\mathrm{i}=1}^{N} x^{\mathrm{k}}{}_{\mathrm{i}} \left[y_{\mathrm{i}} - \sum_{\mathrm{r}=0}^{\mathrm{q}} \hat{a}_{\mathrm{r}} x_{\mathrm{i}}{}^{\mathrm{r}} \right] = 0 \qquad \mathrm{k} = 0, 1, 2, \ldots, \mathrm{q}. \tag{A.1}$$

Defining the Vandermonde matrix

$$\mathbf{C} \equiv \begin{pmatrix} 1 & x_1 & {x_1}^2 & {x_1}^3 & \ldots & {x_1}^{\mathrm{q}} \\ 1 & x_2 & {x_2}^2 & {x_2}^3 & \ldots & {x_2}^{\mathrm{q}} \\ \vdots & \vdots & \vdots & \vdots & & \vdots \\ 1 & x_N & {x_N}^2 & {x_N}^3 & \ldots & {x_N}^{\mathrm{q}} \end{pmatrix} ,$$

and

$$\mathbf{y} \equiv \begin{pmatrix} y_1 \\ y_2 \\ \vdots \\ y_N \end{pmatrix},$$

permits one to rewrite the normal equations (A.1) in matrix form

$$\mathbf{C}^{\mathrm{T}}\left[\mathbf{y} - \mathbf{C}\hat{\mathbf{a}}\right] = 0\,,$$

which, in principle, easily can be solved for $\hat{\mathbf{a}}$

$$\hat{\mathbf{a}} = \left(\mathbf{C}^{\mathrm{T}}\mathbf{C}\right)^{-1}\mathbf{C}^{\mathrm{T}}\mathbf{y}\,. \tag{A.2}$$

Equidistant x values Now suppose equidistant x values. In order to facilitate coming computations all x values are shifted by an amount which results in symmetric x values. That is: If N is odd the x values are shifted to

$$0, \quad \pm\Delta, \quad \pm 2\Delta, \quad \pm 3\Delta, \quad \ldots, \quad , \pm\frac{N-1}{2}\Delta\,,$$

and if N is even the x values are shifted to

$$\pm\frac{\Delta}{2}, \quad \pm\frac{3\Delta}{2}, \quad \pm\frac{5\Delta}{2}, \quad \pm\frac{7\Delta}{2}, \quad \ldots, \quad \pm\frac{N-1}{2}\Delta\,.$$

Consequently, the mean value of x to the power of odd integers vanishes

$$\frac{1}{N}\sum_{\mathrm{i}=1}^{N} {x_{\mathrm{i}}}^{\mathrm{k}} = 0 \qquad \mathrm{k\ odd}\,.$$

A.2.1 Linear least squares

Consider the simplest case of fitting a straight line[1], $f(x;\mathrm{a}) = \mathrm{a}_0 + \mathrm{a}_1 x$, to N equidistant points. Matrix $\mathbf{C}$ is given by

$$\mathbf{C} = \begin{pmatrix} 1 & x_1 \\ 1 & x_2 \\ \vdots & \vdots \\ 1 & x_N \end{pmatrix} .$$

After some matrix multiplications, equation (A.2) takes the form

$$\hat{\mathbf{a}} = \underbrace{\begin{pmatrix} 1 & \overline{x} \\ \overline{x} & \overline{x^2} \end{pmatrix}^{-1}}_{\mathbf{C}^{\mathrm{T}}\mathbf{C}} \underbrace{\begin{pmatrix} \overline{y} \\ \overline{xy} \end{pmatrix}}_{\mathbf{C}^{\mathrm{T}}\mathbf{y}}, \tag{A.3}$$

where $\overline{(\,)}$ denotes the mean value

$$\overline{(\,)} \equiv \frac{1}{N}\sum_{\mathrm{i}=1}^{N}(\,) .$$

Shifting the x values as described in section A.2 makes the mean value of x vanish. Consequently, equation (A.3) can be rewritten as

$$\hat{\mathbf{a}} = \begin{pmatrix} 1 & 0 \\ 0 & 1/\overline{x^2} \end{pmatrix} \begin{pmatrix} \overline{y} \\ \overline{xy} \end{pmatrix} ,$$

after a trivial matrix inversion. For $N = 3$ the linear least squares fit is given by[2]

$$y = \overline{y} - \frac{y_1 - y_3}{2}\left(\frac{x}{\Delta}\right) .$$

---

[1] q=1

[2] $\overline{x^2} = \frac{2}{3}\Delta^2$ and $\overline{xy} = \frac{1}{3}\left(-\Delta y_1 + \Delta y_3\right)$

A.2.2 Quadratic least squares

Fitting a parabola, $f(x;\mathrm{a}) = \mathrm{a}_0 + \mathrm{a}_1 x + \mathrm{a}_2 x^2$, to N equidistant data points is a straight forward extension of the first order polynomial fit explained in section A.2.1. However, inversion of the matrix $\mathbf{C}^{\mathrm{T}}\mathbf{C}$ is no longer trivial despite the high degree of symmetry and regularity in its structure.

Matrix $\mathbf{C}$ is given by

$$\mathbf{C} = \begin{pmatrix} 1 & x_1 & x_1^2 \\ 1 & x_2 & x_2^2 \\ \vdots & \vdots & \vdots \\ 1 & x_N & x_N^2 \end{pmatrix}.$$

Equation (A.2) takes the form

$$\hat{\mathbf{a}} = \underbrace{\begin{pmatrix} 1 & 0 & \overline{x^2} \\ 0 & \overline{x^2} & 0 \\ \overline{x^2} & 0 & \overline{x^4} \end{pmatrix}^{-1}}_{\frac{1}{N}\mathbf{C}^{\mathrm{T}}\mathbf{C}} \underbrace{\begin{pmatrix} \overline{y} \\ \overline{xy} \\ \overline{x^2 y} \end{pmatrix}}_{N\mathbf{C}^{\mathrm{T}}\mathbf{y}},$$

after performing the x-axis shift which makes $\overline{x}$ and $\overline{x^3}$ vanish. The inverse can be written as

$$\left(\mathbf{C}\mathbf{C}^{\mathrm{T}}\right)^{-1} = \frac{N}{\overline{x^2}\,\overline{x^4} - \overline{x^2}^3} \cdot \begin{pmatrix} \overline{x^2}\,\overline{x^4} & 0 & -\overline{x^2}^{\,2} \\ 0 & \overline{x^4} - \overline{x^2}^{\,2} & 0 \\ -\overline{x^2}^{\,2} & 0 & \overline{x^2} \end{pmatrix}. \tag{A.4}$$

For $N = 4$ we have

$$\begin{aligned}
\overline{x^2} &= \frac{5}{4}\Delta^2, \\
\overline{x^4} &= \frac{41}{16}\Delta^4, \\
\overline{xy} &= \frac{\Delta}{8}\left(-3y_1 - y_2 + y_3 + 3y_4\right), \\
\overline{x^2 y} &= \frac{\Delta^2}{16}\left(9y_1 + y_2 + y_3 + 9y_4\right).
\end{aligned}$$

By insertion in equation (A.4), and after performing the matrix multiplications, one obtains the coefficients for the least squares parabola fit

$$\begin{aligned}
\hat{a}_0 &= \frac{1}{16}\left(-y_1 + 9y_2 + 9y_3 - y_4\right), \\
\hat{a}_1 &= \frac{1}{10}\frac{1}{\Delta}\left(-3y_1 - y_2 + y_3 + 3y_4\right), \\
\hat{a}_2 &= \frac{1}{4}\frac{1}{\Delta^2}\left(y_1 - y_2 - y_3 + y_4\right).
\end{aligned}$$

A.2.3 Cubic and quartic least squares

Extension to the cubic and quartic cases is in principle a straight forward extension of the linear and quadratic cases. The calculations are quite lengthy, therefore only the results are given. A four point least squares fit to a cubic polynomial, $f(x;\mathrm{a}) = \mathrm{a}_0 + \mathrm{a}_1 x + \mathrm{a}_2 x^2 + \mathrm{a}_3 x^3$, yields the coefficients

$$\begin{aligned}
\hat{a}_0 &= \frac{1}{35}\left(-3y_1 + 12y_2 + 17y_3 + 12y_4 - 3y_5\right), \\
\hat{a}_1 &= \frac{1}{12}\frac{1}{\Delta}\left(y_1 - 8y_2 + 8y_4 - y_5\right), \\
\hat{a}_2 &= \frac{1}{14}\frac{1}{\Delta^2}\left(2y_1 - y_2 - 2y_3 - y_4 + 2y_5\right), \\
\hat{a}_3 &= \frac{1}{12}\frac{1}{\Delta^3}\left(-y_1 + 2y_2 - 2y_4 + y_5\right).
\end{aligned}$$

Similarly, performing a least squares fit with a quartic polynomial, $f(x;\mathrm{a}) = \mathrm{a}_0 + \mathrm{a}_1 x + \mathrm{a}_2 x^2 + \mathrm{a}_3 x^3 + \mathrm{a}_4 x^4$, to five points yields the coefficients

$$\begin{aligned}
\hat{a}_0 &= \frac{1}{256}\left(3y_1 - 25y_2 + 150y_3 + 150y_4 - 25y_5 + 3y_6\right) , \\
\hat{a}_1 &= \frac{1}{3024}\frac{1}{\Delta}(275y_1 - 1249y_2 - 652y_3 + 652y_4 + 1249y_5 - 275y_6) , \\
\hat{a}_2 &= \frac{1}{96}\frac{1}{\Delta^2}\left(-5y_1 + 39y_2 - 34y_3 - 34y_4 + 39y_5 + 5y_6\right) , \\
\hat{a}_3 &= \frac{1}{108}\frac{1}{\Delta^3}\left(-5y_1 + 7y_2 + 4y_3 - 4y_4 - 7y_5 + 5y_6\right) , \\
\hat{a}_4 &= \frac{1}{48}\frac{1}{\Delta^4}\left(y_1 - 3y_2 + 2y_3 + 2y_4 - 3y_5 + y_6\right) .
\end{aligned}$$

Conversion In order to convert the formulas to the notation of the semi-Lagrangian framework one needs to revert the x-axis and replace x by $\hat{\alpha}\Delta$. That is to perform the transformation

$$x \to -\hat{\alpha}\Delta .$$

Of course y_j has to be replaced by an appropriate ϕ. For example, in the linear least squares case y_1, y_2 and y_3 are replaced by ϕ^n_{I-p-1}, ϕ^n_{I-p} ϕ^n_{I-p+1}, respectively.

A.2.4 Weighted least squares

To do a weighed least squares fit we associate an weight, $\frac{1}{\sigma_i}$, to each grid point value, y_i. To obtain the coefficients of a weighted fit minimize

$$\sum_{\mathrm{i}=1}^{N}\left[\frac{y_\mathrm{i} - f\left(x_\mathrm{i};\mathbf{a}\right)}{\sigma_i}\right]^2 .$$

Following the same method as outlined for the non-weighted least squares fit, the solution is given by

$$\hat{\mathbf{a}} = \left(\mathbf{C}^{\mathrm{T}}\mathbf{V}\mathbf{C}\right)^{-1}\mathbf{C}^{\mathrm{T}}\mathbf{V}\mathbf{y} ,$$

where $\mathbf{V}$ is a diagonal matrix containing the squared weights

$$\mathbf{V} \equiv \begin{pmatrix} \frac{1}{\sigma_1^2} & & & \\ & \frac{1}{\sigma_2^2} & & \\ & & \ddots & \\ & & & \frac{1}{\sigma_N^2} \end{pmatrix}.$$

A.3 Detailed amplification factor computations

Here are some of the computations leading to the formulas for amplification factors of least squares schemes listed in table 2.2.

Seeking a solution

$$\phi_j^n = \Gamma^n \exp(i\, j\delta)\, \phi^0 ,$$

the substitution into the finite difference schemes given in table 2.1 yields

$$\Gamma^{(1)} = e^{-ip\delta} \left\{ \tfrac{1}{3}(1 + 2\cos\delta) - i\,\hat{\alpha}\sin\delta \right\} ,$$
$$\Gamma^{(3)} = e^{-ip\delta} \left\{ 1 - c\left(\hat{\alpha}^2 - c\left(-\tfrac{12}{35} + \tfrac{4}{7}\hat{\alpha}^2\right)\right) + i\,\hat{\alpha}\sin\delta\left(-1 + \tfrac{1}{3}c\left(\hat{\alpha}^2 - 1\right)\right) \right\} ,$$

where $\Gamma^{(1)}$ refers to Γ of the straight line fit and $\Gamma^{(3)}$ refers to the cubic case. For the quadratic and quartic schemes we have

$$\Gamma^{(2)} = e^{-ip\delta} \left\{ 1 - \mathcal{D}^2 c + \mathcal{G} c^2 + i\ (-\mathcal{D} + \mathcal{G} c)\sin\delta \right\} ,$$

and

$$\Gamma^{(4)} = e^{-ip\delta} \left\{ 1 - \mathcal{D}^2\, c + \tfrac{1}{4}\mathcal{E}\, c^2 + \mathcal{F}\, c^3 + i\ \left(-\mathcal{D} + \mathcal{E}\, c + \mathcal{F}\, c^2\right)\sin\delta \right\} ,$$

respectively, where

$$\mathcal{D} = \tfrac{1}{2} + \hat{\alpha} ,$$
$$\mathcal{E} = \tfrac{1}{24}(3 + 2\hat{\alpha})(1 + 2\hat{\alpha})(-1 + 2\hat{\alpha}) ,$$
$$\mathcal{F} = -\tfrac{3}{64} + \tfrac{275}{756}\hat{\alpha} + \tfrac{5}{24}\hat{\alpha}^2 - \tfrac{5}{27}\hat{\alpha}^3 - \tfrac{1}{12}\hat{\alpha}^4 ,$$
$$\mathcal{G} = \tfrac{1}{40}\left(-5 + 24\hat{\alpha} + 20\hat{\alpha}^2\right) .$$

A.4 Proofs for theorems and lemmas

Proof for lemma 1, chapter 3 To insure unconditional stability we must have that $||\Gamma||^2 \leq 1$ for all values that c and $\hat{\alpha}$ may take. Solving $||\Gamma||^2 = 1$ for A_1 yields

$$A_1^{\pm} = \frac{1}{4}\frac{2c\,\hat{\alpha} + 2 \pm 2\sqrt{c^2\hat{\alpha}^2 + 1 - 2c\,\hat{\alpha}^2}}{c}.$$

For fixed $(\hat{\alpha}, c)$ and having A_1 confined to the interval bounded by A_1^- and A_1^+ will guarantee unconditional stability[3]. As the value of c can take any value in between 0 and 2, the lemma is proved by minimizing the upper bound of A_1 and maximizing the lower bound of A_1 with respect to c. It can easily be verified that $A_1^{\pm}$ is monotonic and decreasing on the domain of interest. That is

$$\frac{\partial A_1^{\pm}}{\partial c} \leq 0 \qquad \text{for } (c, \hat{\alpha}) \in \ ]0, 2] \times \left[-\tfrac{1}{2}, \tfrac{1}{2}\right[.$$

Therefore the maximum/(minimum) unconditional stable value of A_1 is obtained for $c = 2/(c = 0)$. Calculating A_1^+ with $c = 2$ and A_1^- with $c = 0$ completes the proof.

□

Proof for theorem 2, chapter 3 Write out the sum of the left hand side using (3.3) and periodic boundary conditions for some fixed p and M value. For example for $p = 0$ and $M = 5$ we have

$$\begin{array}{ccccccc}
A_1\phi_4 & + & A_2\phi_0 & + & A_3\phi_1 & + \\
A_1\phi_0 & + & A_2\phi_1 & + & A_3\phi_2 & + \\
A_1\phi_1 & + & A_2\phi_2 & + & A_3\phi_3 & + \\
A_1\phi_2 & + & A_2\phi_3 & + & A_3\phi_4 & + \\
A_1\phi_3 & + & A_2\phi_4 & + & A_3\phi_0 & .
\end{array}$$

[3] calculating $||\Gamma||^2$ for any allowed $(\hat{\alpha}, c)$ value and any A_1 in $\left[A_1^-, A_1^+\right]$ will yield a value less than or equal to unity. Choosing A_1 outside $\left[A_1^-, A_1^+\right]$ yields a value greater than one. Continuity then proves the statement

Collecting terms (diagonal) and using the necessary condition for consistency (3.6) proofs the theorem[4]. □

[4]the theorem may easily be extended to N point schemes

A.5 List of explicit formulas for higher order schemes

Here is a list of explicit formulas for quantities used in the higher order analysis (section 3.3). In all the following formulas $\hat{\alpha}$, p, c and δ are defined as in section 3.1.1.

A.5.1 Lagrange interpolation, $\mathcal{L}$

For the four point scheme, $N = 4$, the Lagrange interpolation using ϕ^n_{I-p-1}, ϕ^n_{I-p} and ϕ^n_{I-p+1} is given by

$$\mathcal{L} = \tfrac{1}{2}\hat{\alpha}(1+\hat{\alpha})\,\phi^n_{I-1} + (1-\hat{\alpha}^2)\,\phi^n_I - \tfrac{1}{2}\hat{\alpha}(1-\hat{\alpha})\,\phi^n_{I+1}\,.$$

For the five point scheme, $N = 5$, the Lagrange interpolation using ϕ^n_{I-p-1}, ϕ^n_{I-p}, ϕ^n_{I-p+1} and ϕ^n_{I-p+2} is given by

$$\begin{aligned}\mathcal{L} = \frac{1}{6}\,\hat{\alpha}\,(\hat{\alpha}+2)\,(\hat{\alpha}+1)\,\phi^n_{I-1} - \frac{1}{2}\,\left(\hat{\alpha}^2-1\right)\,(\hat{\alpha}+2)\,\phi^n_I \\ + \frac{1}{2}\,\hat{\alpha}\,(\hat{\alpha}+2)\,(\hat{\alpha}-1)\,\phi^n_{I+1} - \frac{1}{6}\,\hat{\alpha}\,\left(\hat{\alpha}^2-1\right)\,\phi^n_{I+2}\,.\end{aligned}$$

For the six point scheme, $N = 6$, the Lagrange interpolation using ϕ^n_{I-p-2}, ϕ^n_{I-p-1}, ϕ^n_{I-p}, ϕ^n_{I-p+1} and ϕ^n_{I-p+2} is given by

$$\begin{aligned}\mathcal{L} = \tfrac{1}{24}\,\hat{\alpha}\,\left(\hat{\alpha}^2-1\right)\,(\hat{\alpha}+2)\,\phi^n_{I-2} - \tfrac{1}{6}\,\hat{\alpha}\,\left(\hat{\alpha}^2-4\right)\,(\hat{\alpha}+1)\,\phi^n_{I-1} \\ + \tfrac{1}{4}\,\left(\hat{\alpha}^2-1\right)\,\left(\hat{\alpha}^2-4\right)\,\phi^n_I \\ - \tfrac{1}{6}\,\hat{\alpha}\,(\hat{\alpha}-1)\,\left(\hat{\alpha}^2-4\right)\,\phi^n_{I+1} + \tfrac{1}{24}\,\hat{\alpha}\,\left(\hat{\alpha}^2-1\right)\,(\hat{\alpha}-2)\,\phi^n_{I+2}\,.\end{aligned}$$

A.5.2 The amplification factors of higher order schemes

The squared modulus of the amplification factor is split into a part associated with the Lagrange interpolation, $\mathcal{L}$, and a rest term $\mathcal{R}$ (see section 3.3.2 for details)

$$||\Gamma||^2 = ||\Gamma_{\mathcal{L}}||^2 + ||\Gamma_{\mathcal{R}}||^2\,.$$

The squared amplification associated with the Lagrange Interpolation, $||\Gamma_{\mathcal{L}}||^2$, is given by

$$||\Gamma_{\mathcal{L}}||^2 = \begin{cases} 1 - \quad c^2\,\hat{\alpha}^2\,(1-\hat{\alpha}^2) & \text{for} \quad N=4 \\ 1 - \frac{1}{3}\,c^2\,\hat{\alpha}\;\;(1-\hat{\alpha}^2)\,(2+\hat{\alpha})\;\;\left[1-\frac{2}{3}\,c\,\hat{\alpha}^2\,(1+\hat{\alpha})\right] & \text{for} \quad N=5 \\ 1 - \frac{1}{9}\,c^3\,\hat{\alpha}^2\,(1-\hat{\alpha}^2)\,(4-\hat{\alpha}^2)\left[1-\frac{1}{4}\,c\,(\hat{\alpha}^2-1)\right] & \text{for} \quad N=6. \end{cases}$$

The rest term, $||\Gamma_{\mathcal{R}}||^2$, is given by

$$||\Gamma_{\mathcal{R}}||^2 = \begin{cases} 4\,A_1\,c^2\left[1+2\,A_1\,c\;\;-\hat{\alpha}^2\,c-2\,\hat{\alpha}+c\,\hat{\alpha}\right] & \text{for} \quad N=4 \\ 8\,A_1\,c^2\left[1+2\,A_1\,c^2-\hat{\alpha}^2\,c-\frac{1}{3}\,\hat{\alpha}\,(\hat{\alpha}^2-1)\,c^2\right] & \text{for} \quad N=5 \\ -8\,A_1\,c^3\left[1-4\,A_1\,c^2-2\,\hat{\alpha}+\frac{1}{3}\,\hat{\alpha}\,(2\,\hat{\alpha}-1)\,(\hat{\alpha}-1)\,c\right. & \\ \qquad\qquad\left.+\frac{1}{6}\,\hat{\alpha}\,(\hat{\alpha}^2-1)\,(\hat{\alpha}-2)\,c^2\right] & \text{for} \quad N=6. \end{cases}$$

A.5.3 Unconditionally stable interval, $[A^-, A^+]$

The interval of A_1 values yielding unconditionally stable schemes has lower bound, A^-, given by

$$A^- = \begin{cases} \frac{1}{4}\,(\hat{\alpha}^2-1) & \text{for} \quad N=4 \\ \frac{1}{24}\,(\hat{\alpha}^2-1)\,(2\,\hat{\alpha}+3) & \text{for} \quad N=5 \\ \frac{1}{48}\,\hat{\alpha}^2\,(\hat{\alpha}^2-4) & \text{for} \quad N=6\,, \end{cases}$$

and upper bound, A^+, given by

$$A^+ = \begin{cases} \frac{1}{4}\,\hat{\alpha}^2 & \text{for} \quad N=4 \\ \frac{1}{24}\,\hat{\alpha}\,(\hat{\alpha}^2-1)\,(2+\hat{\alpha}) & \text{for} \quad N=5 \\ \frac{1}{48}\,(\hat{\alpha}^2-1)\,(\hat{\alpha}^2-3) & \text{for} \quad N=6. \end{cases}$$

A.5.4 The A_1 value for which the 2Δ wave is completely damped, A^*

Solving $||\Gamma||^2 = 0$ for the 2Δ wave yields an A_1 value, A^*, given by

$$A^* = \begin{cases} \frac{1}{4}\left(\hat{\alpha}^2 - \frac{1}{2}\right) & \text{for} \quad N = 4 \\ \frac{1}{48}\,(2\,\hat{\alpha}+1)\,(2\,\hat{\alpha}^2 + 2\,\hat{\alpha} - 3) & \text{for} \quad N = 5 \\ \frac{1}{32} - \frac{1}{12}\,\hat{\alpha}^2 + \frac{1}{48}\,\hat{\alpha}^4 & \text{for} \quad N = 6. \end{cases}$$

A.5.5 Least squares value of A_1, $A^{\mathcal{LS}}$

For schemes using an even number of points for interpolation the definition of $\hat{\alpha}$ has been redefined in chapter 3. Therefore the coefficients from table 2.1 from the least squares analysis need to be shifted using the following transform: $\hat{\alpha} \rightarrow \hat{\alpha} - \frac{1}{2}$ (N even). For N odd the definition of $\hat{\alpha}$ in the least squares analysis and in the analysis of the more general scheme are identical. The A_1 values yielding $(N-2)$th-order least squares schemes are given by

$$A^{(N-2)\,\mathcal{LS}} = \begin{cases} -\frac{3}{20} + \frac{1}{20}\,\hat{\alpha} + \frac{1}{4}\,\hat{\alpha}^2 & \text{for} \quad N = 4 \\ \mathcal{A}_+^{(3)} & \text{for} \quad N = 5 \\ \frac{5}{126} - \frac{11}{756}\,\hat{\alpha} - \frac{13}{144}\,\hat{\alpha}^2 + \frac{1}{216}\,\hat{\alpha}^3 + \frac{1}{48}\,\hat{\alpha}^4 & \text{for} \quad N = 6. \end{cases}$$

where the superscript $(N-2)$ has to be replaced by the value of N-2.

A.5.6 The A_1 value yielding the $(N-1)$th-order conventional semi-Lagrangian scheme

Given N, the A_1 value yielding maximum order of accuracy, is the A_1 value generating the $(N-1)$-th order conventional semi-Lagrangian scheme. This A_1 is given by

$$A^{(N-1)\,cL} = \begin{cases} \frac{1}{6}\,(\hat{\alpha}^2-1) & \text{for} \quad N=4 \\ A^{+} & \text{for} \quad N=5 \\ \frac{1}{120}\,\hat{\alpha}\,(\hat{\alpha}^2-1)\,(\hat{\alpha}^2-4) & \text{for} \quad N=6\,, \end{cases}$$

where the superscript $(N-1)$ has to be replaced by the value of N-1.

A.5.7 The A_1 value yielding the $(N-2)$th-order conventional semi-Lagrangian scheme

The $(N-2)$th-order conventional semi-Lagrangian schemes uses $(N-1)$ points for the interpolation. Hence either A_1 or A_N must equal zero. As it may be deduced from footnote 8 on page 45, an A_1 value yielding the $(N-2)$th-order conventional semi-Lagrangian scheme does not exist for all $\hat{\alpha}$ values since the central grid point for the interpolation, x_{I-p}, not always corresponds to the one used in a conventional semi-Lagrangian scheme. For N even and $\hat{\alpha} \leq \frac{1}{2}$ a vanishing A_1 value, $A_1 = 0$, will yield the $(N-2)$th-order conventional semi-Lagrangian scheme. For $\hat{\alpha} > \frac{1}{2}$ no value of A_1 will yield the $(N-2)$th-order conventional semi-Lagrangian scheme ("wrong" central grid point for interpolation). For N odd and $\hat{\alpha}$ positive, solving $A_N = 0$ for A_1 will yield the $(N-2)$th-order conventional semi-Lagrangian scheme. For $N=5$ we have

$$A^{3cL} = \begin{cases} \frac{1}{6}\,\hat{\alpha}\,(\hat{\alpha}^2-1) & \text{for} \quad \hat{\alpha} \geq 0 \\ \text{does not exist} & \text{for} \quad \hat{\alpha} < 0\,. \end{cases}$$

A.5.8 The relative phase speeds of higher order schemes

The relative phase speed, R, is given by

$$R = \frac{1}{\delta\,(p+\hat{\alpha})} \begin{cases} \delta p + \arctan\left(\frac{(\hat{\alpha}-2\,A_1 c)\,\sin\delta}{1-c\,(\hat{\alpha}^2-2\,A_1 c)}\right) & \text{for} \quad N=4 \\ \delta p + \arctan\left(\frac{\left(\hat{\alpha}+\frac{1}{3}\,\hat{\alpha}\left(1-\hat{\alpha}^2\right)\right)\,\sin\delta}{1-\hat{\alpha}^2\,c+\left(\frac{1}{3}\,\hat{\alpha}(1-\hat{\alpha}^2)+4\,A_1\right)c^2}\right) & \text{for} \quad N=5 \\ \delta p + \arctan\left(\frac{\left(\hat{\alpha}+(1-\hat{\alpha})\,c+4\,c^2\,A_1\right)\,\sin\delta}{1-4\,A_1\,c^3-\hat{\alpha}^2\,c+\frac{1}{6}\,\hat{\alpha}\,c^2\,(\hat{\alpha}^2-1)}\right) & \text{for} \quad N=6. \end{cases}$$

A.5.9 Relative phase speed of the 2Δ wave

Define the limit values R^+ and R^- by

$$R^+ \equiv \frac{p+\mathrm{sgn}(\hat{\alpha})}{p+\hat{\alpha}}\,,$$

and

$$R^- \equiv \frac{p}{p+\hat{\alpha}}\,,$$

where sgn() is the signum function. In the special case of $\hat{\alpha}=0$ would need to be treated separately. However, as discussed in section 2.4, an interpolation method with the cardinal property is preferred.

For $N=4$ and $N=5$ the relative phase speed, R, converges to

$$\begin{array}{ll} R^+ & \text{for} \quad A_1 < A^*\,, \\ R^- & \text{for} \quad A_1 > A^*\,, \end{array} \tag{A.5}$$

in the 2Δ wave limit. Note that for a fixed departure point, x_*, the $\hat{\alpha}$ value of the four and five point schemes may not be identical. Consequently, $R^\pm$ of the four point scheme is not necessarily equal to $R^\pm$ of the five point scheme. For $N=6$ R converges

to

$$\begin{array}{ll} R^+ & \text{for} \quad A_1 > A^*\,, \\ R^- & \text{for} \quad A_1 < A^*\,, \end{array} \tag{A.6}$$

for $\delta \to 2$.

Bibliography

[Bates and McDonald, 1982] Bates, J. and McDonald, A. (1982). Multiply-upstream, semi-lagrangian advective schemes: Analysis and application to a multi-level primitive equation model. *Monthly Weather Review*, 110:1831–1842.

[Bermejo, 1990] Bermejo, R. (1990). Notes and correpondence on the equivalence of semi-lagrangian schemes and particle-in-cell finite element methods. *Monthly Weather Review*, 118:979–987.

[Bermejo and Staniforth, 1992] Bermejo, R. and Staniforth, A. (1992). The conversion of semi-lagrangian advection schemes to quasi-monotone schemes. *Monthly Weather Review*, 120:2622–2632.

[Durran, 1998] Durran, D. (1998). *Numerical Methods for Wave Equations in Geophysical Fluid Dynamics*. Springer.

[Godunov, 1959] Godunov, S. (1959). A difference scheme for numerical computation of discontinous solutions of equations in fluid dynamics. *Math. Sb.*, 47:271–290.

[Holnicki, 1995] Holnicki, P. (1995). A shape-preserving interpolation: Applications to semi-lagrangian advection. *Monthly Weather Review*, 123:862–870.

[Lin and Rood, 1996] Lin, S. and Rood, R. (1996). Multidimensional flux-form semi-lagrangian transport schemes. *Monthly Weather Review*, 124:2046–2070.

[McDonald, 1984] McDonald, A. (1984). Accuracy of multiply-upstream, semi-lagrangian advective schemes. *Monthly Weather Review*, 112:1267–1275.

[Ostiguy and Laprise, 1990] Ostiguy, L. and Laprise, J. (1990). On the positivity of mass in commonly used numerical transport schemes. *Atmosphere-Ocean*, 28(2):147–161.

[Priestly, 1993] Priestly, A. (1993). A quasi-conservative version of the semi-lagrangian advections scheme. *Monthly Weather Review*, 121:621–629.

[Purnell, 1976] Purnell, D. (1976). Solution of the advective equation by upstream interpolation with cubic splines. *Monthly Weather Review*, 104:42–48.

[Rancic, 1992] Rancic, M. (1992). Semi-lagrangian piecewise biparabolic scheme for two-dimensional horizontal advection of a passive scalar. *Monthly Weather Review*, 120:1394–1405.

[Rancic, 1995] Rancic, M. (1995). An efficient, conservative, monotonic remapping for semi-lagrangian transport algorithms. *Monthly Weather Review*, 123:1213–1217.

[Rasch and Williamson, 1990] Rasch, P. and Williamson, D. (1990). Computational aspects of moisture transport in global models of the atmosphere. *Q.J.R.Metorol.Soc.*, 116:1071–1090.

[Riishjgaard et al., 1998] Riishjgaard, L., Cohn, S., and Menard, R. (1998). The use of spline interpolation in semi-lagrangian transport models. *Monthly Weather Review*, 126:2008–2016.

[Ritchie, 1986] Ritchie, H. (1986). Eliminating the interpolation associated with the semi-lagrangian scheme. *Monthly Weather Review*, pages 135–146.

[Robert, 1981] Robert, A. (1981). A numerical integration scheme for the primitive meorological equations. *Atmosphere-Ocean*, 19:36–45.

[Rood, 1987] Rood, R. (1987). Numerical advection algorithms and their role in atmospheric transport and chemistry models. *Review of Geophysics*, 25(1):71–100.

[Smolarkiewicz and Gabowski, 1990] Smolarkiewicz, P. and Gabowski, W. (1990). The multidimensional positive definite advection transport algorithm: Nonoscillatory option. *Journal of Computational Physics*, 86:355–375.

[Smolarkiewicz and Pudykiewicz, 1992] Smolarkiewicz, P. and Pudykiewicz, J. (1992). A class of semi-lagrangian approximations for fluids. *Journal of the Atmospheric Sciences*, 49(22):2082–2096.

[Staniforth and Côté, 1991] Staniforth, A. and Côté, J. (1991). Semi-lagrangian schemes for atmospheric models-a review. *Monthly Weather Review*, 119:2206–2223.

[Takacs, 1985] Takacs, L. (1985). A two-step scheme for the advection equation with minimized dissipation and dipsersion errors. *Monthly Weather Review*, 113:1050–1065.

[WCRP, 1990] WCRP (1990). *Collection of papers presented at the WCRP Symposium on Global Tracer Transport Models (Bermuda)*, Available from Dr.V.Savtchenko, WMO, C.P.2300, CH 1211, Geneva 2, Switzerland.

[Williamson and Rasch, 1989] Williamson, D. and Rasch, P. (1989). Two-dimensional semi-lagrangian transport with shape-preserving interpolation. *Monthly Weather Review*, 117:102–129.

[Yabe et al., 2001] Yabe, T., Tanaka, R., Nakamura, T., and Xiao, F. (2001). An exactly conservative semi-lagrangian scheme (cip csl) in one dimension. *Monthly Weather Review*, 129.